



Preliminary Gap Analysis of Existing IEEE 1547 and IEEE 2800 Standards Towards GFM Technology

Deepak Ramasubramanian,¹ Wenzong Wang,¹ Wes Baker,¹
Mohammad (Aminul) Huque,¹ Jens C. Boemer,¹
Rodrigo H. Auba,² Dustin Howard,³ and Ganesh Marasini⁴

1 Electric Power Research Institute

2 University of California, Berkeley

3 GE Energy Consulting

4 Student intern

NREL Technical Monitor: Ben Kroposki

Suggested Citation

Ramasubramanian, D., et al. 2022. *Preliminary Gap Analysis of Existing IEEE 1547 and IEEE 2800 Standards Towards GFM Technology*. UNIFI-2022-3-1.

The Universal Interoperability for Grid-Forming Inverters (UNIFI) Consortium is co-led by the National Renewable Energy Laboratory, the University of Texas-Austin, and the Electric Power Research Institute. This material is based upon work supported by the U.S. Department of Energy's Office of Energy Efficiency and Renewable Energy (EERE) under the Solar Energy Technologies Office Award Number 38637.



DISCLAIMER

This report was prepared as an account of work sponsored by an agency of the United States Government. Neither the United States Government nor any agency thereof, nor any of their employees, makes any warranty, express or implied, or assumes any legal liability or responsibility for the accuracy, completeness, or usefulness of any information, apparatus, product, or process disclosed, or represents that its use would not infringe privately owned rights. Reference herein to any specific commercial product, process, or service by trade name, trademark, manufacturer, or otherwise does not necessarily constitute or imply its endorsement, recommendation, or favoring by the United States Government or any agency thereof. The views and opinions of authors expressed herein do not necessarily state or reflect those of the United States Government or any agency thereof.

This report is available at no cost from the National Renewable Energy Laboratory (NREL) at www.nrel.gov/publications.

U.S. Department of Energy (DOE) reports produced after 1991 and a growing number of pre-1991 documents are available free via www.OSTI.gov.

NREL prints on paper that contains recycled content.

**NREL is a national laboratory of the U.S. Department of Energy
Office of Energy Efficiency & Renewable Energy
Operated by the Alliance for Sustainable Energy, LLC**

This report is available at no cost from the National Renewable Energy Laboratory (NREL) at www.nrel.gov/publications.

Contract No. DE-AC36-08GO28308

Technical Report
NREL/TP-5D00-88609
February 2024

National Renewable Energy Laboratory
15013 Denver West Parkway
Golden, CO 80401
303-275-3000 • www.nrel.gov

Executive Summary

This document describes the tests that are conducted on generic grid-forming (GFM) distributed energy resource (DER) and inverter-based resource (IBR) models to check if the performance of the model aligns respectively with the IEEE Std 1547TM-2018 and IEEE Std 2800TM-2022 requirements.

For the IEEE Std 1547TM-2018 requirements, specifically the tests related to volt-var requirements and frequency droop requirements are conducted.

For the IEEE Std 2800TM-2022 requirements, specifically the tests conducted are related to reactive- power-voltage control requirements, active-power-frequency response requirements, voltage disturbance ride through requirements and phase jump ride through requirements.

This is an initial draft/document. There are many more tests still yet to be done to further verify if the existing standards have a gap or inadvertent barrier to GFM technology.

Table of Contents

- Executive Summary** **iii**
- List of Figures** **v**
- List of Tables** **vi**
- Introduction** **1**
- IEEE 1547-2018 Tests** **5**
 - Volt-Var test 5
 - Test criteria 5
 - Test system 6
 - Test results 7
 - Frequency-droop test 12
- IEEE 2800-2022 Tests** **17**
 - Reactive power-voltage control test 17
 - Active power-frequency response test 20
 - Low voltage ride-through response test 24
 - Voltage phase angle change test 31
- Summary** **44**
- References** **45**

List of Figures

Figure 1. Structure of generic positive sequence grid forming model to capture structural and operational similarity across four different grid forming methods	2
Figure 2. Volt-Var droop as per IEEE Std 1547 TM -2018.....	5
Figure 3. Test system for generic GFM model.....	7
Figure 4. Test system for GFL inverter	7
Figure 5. Response of generic GFM model and GFL inverter for a step change in AC source voltage within continuous operation region	9
Figure 6. Response of generic GFM model and GFL inverter for a step change in AC source voltage within mandatory operation region	11
Figure 7. Volt-Var result curve for SRF-PLL GFM control mode	12
Figure 8. Response of generic GFM inverter and GFL inverter for a step change in the frequency of AC source	15
Figure 9. Frequency watt curve for SRF-PLL	16
Figure 10. Test system for voltage-reactive power control test.....	18
Figure 11. Generic GFM model output for a step decrease in source voltage at $t = 5$ s	19
Figure 12. generic GFM model output for step decrease in source voltage at $t = 5$ s.....	20
Figure 13. Response of GFM model for decrease in applicable frequency with ROCOF of 3 Hz/s.....	23
Figure 14. Response of GFM model for increase in applicable frequency with ROCOF of 3 Hz/s.....	24
Figure 15. POC voltage during LG fault	26
Figure 16. Positive sequence active current.....	26
Figure 17. Positive sequence reactive current	27
Figure 18. Negative sequence active current	27
Figure 19. Negative sequence reactive current	28
Figure 20. Phase difference between negative sequence reactive current and negative sequence voltage .	28
Figure 21. POC voltage for balanced LLLG fault	29
Figure 22. Positive sequence active current for balanced LLLG fault.....	30
Figure 23. Positive sequence reactive current for balanced LLLG fault	30
Figure 24. Balanced phase jump in POM voltage	31
Figure 25. Response of GFM model for balanced negative phase jump when $P = 0.1$ p.u., $Q = 0.1$ p.u.....	32
Figure 26. Response of GFM model for balanced negative phase jump when $P = 0.6$ p.u., $Q = 0.1$ p.u.....	33
Figure 27. Response of GFM model for balanced negative phase jump when $P = 0.9$ p.u., $Q = 0.2$ p.u.....	34
Figure 28. balanced positive phase jump in applicable voltage.....	35
Figure 29. Response of GFM model for balanced positive phase jump when $P = 0.1$ p.u., $Q = 0.1$ p.u.....	35
Figure 30. Response of GFM model for balanced positive phase jump when $P = 0.6$ p.u., $Q = 0.1$ p.u.....	36
Figure 31. Response of GFM model for balanced positive phase jump when $P = 0.9$ p.u., $Q = 0.2$ p.u.....	37
Figure 32. Unbalanced phase jump in applicable voltage.....	38
Figure 33. Positive sequence active and reactive current for unbalanced positive phase jump	38
Figure 34. Negative sequence active and reactive current for unbalanced positive phase jump.....	39
Figure 35. Unbalanced phase jump in applicable voltage when $P = 0.1$ p.u. and $Q = 0.1$ p.u.	40
Figure 36. Positive sequence active and reactive current for unbalanced phase jump.....	40
Figure 37. Negative sequence active and reactive current for unbalanced phase jump	41
Figure 38. Positive sequence active and reactive current for unbalanced positive phase jump	42
Figure 39. Negative sequence active and reactive current for unbalanced phase jump	43

List of Tables

Table 1. Default parameters of generic GFM model.....	2
Table 2. IEEE Std 1547TM-2018 voltage-reactive power settings for normal operating performance Category A and Category B DER.....	6
Table 3. Configuration for GFM test system to test volt-var clause.....	8
Table 4. Configuration for GFL test system to test volt-var clause.....	8
Table 5. Open loop response time of different controllers.....	9
Table 6. Configuration for GFL inverter test system for volt-var test.....	10
Table 7. Open loop response time of different controllers.....	11
Table 8. Configuration for GFM test system to test volt-var curve.....	12
Table 7b. Default values and allowable range of frequency droop setting.....	13
Table 8b. Open loop response time of different control modes.....	15
Table 9. Baseline evaluation metrics for voltage-reactive power control mode as per IEEE Std 2800 TM - 2022.....	17
Table 10. Values of various evaluation metrics from response of generic GFM model for a step decrease in applicable voltage.....	19
Table 11. Values of various evaluation matrices for response of generic GFM model for a step decrease in applicable voltage.....	20
Table 12. Parameters for PFR requirements.....	21
Table 13. Evaluation matrices for PFR as per IEEE 2800 TM -2022.....	22
Table 14. Values of various evaluation matrices for GFM model for a decrease in applicable frequency with ROCOF of 3 Hz/s.....	23
Table 15. Values of various evaluation matrices for GFM model for increase in applicable frequency with ROCOF of 3 Hz/s.....	24
Table 16. Performance specification for current injection during voltage ride through events.....	25
Table 17. Values of evaluation metrics for LG fault.....	29
Table 18. Values of performance specifications for LLLG fault.....	30

Introduction

This document describes the tests performed on a generic model of grid-forming (GFM) distributed energy resource (DER) and inverter based resource (IBR). The model of the GFM inverter is generic in the sense that this model can represent four different types of GFM control methods that have been proposed in the literatures. These methods are:

- Phase Locked Loop (SRF-PLL) based GFM control
- Droop based GFM control
- Virtual Synchronous Machine (VSM) based GFM control
- Dispatchable Virtual Oscillator (dVOC) based GFM control

This model is developed in the PSCAD simulation platform. Figure 1 shows the overall structure of the model for a positive sequence representation, but the adaption for EMT representation is straightforward. The default parameters of the model are given in Table 1. The user can switch to the desired GFM control type by appropriately selecting the ω_{flag} parameter. Some of the other parameters in the synchronization elements might also need to be adjusted depending on the control type, but current control parameters can remain the same and are independent of the GFM control selected.

Further details on this model are provided in [1]. Current limits are also represented in the model.

Additionally, for the IBR representation, the model structure has been improved with inclusion of a negative sequence current control functionality to the positive sequence model.

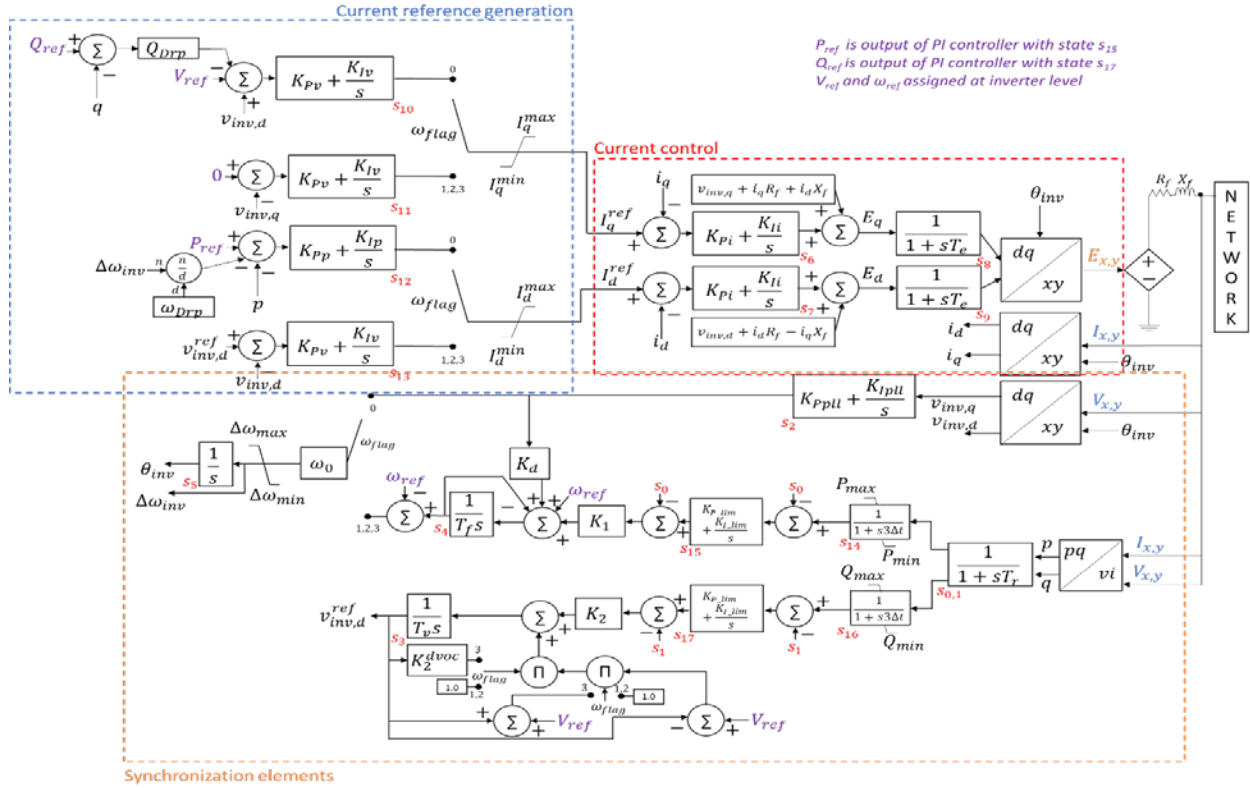


Figure 1. Structure of generic positive sequence grid forming model to capture structural and operational similarity across four different grid forming methods

Table 1. Default parameters of generic GFM model

Parameter	Description	Units	Default Value
MVA rating	IBR rating	MVA	25
R_f	Filter resistance	pu on MVA	0.0015
X_f	Filter reactance	pu on MVA	0.15
V_{dip}	State freeze threshold	pu	0.8
I_{max}	Maximum current magnitude	pu	1.2
PQ flag	Current priority	-	- P priority -Q priority - SRF PLL
ω_{flag}	GFM control type	-	- Droop - VSM 3- dVOC
$\Delta\omega_{max}$	Maximum value of frequency deviation	rad/s	75
$\Delta\omega_{min}$	Minimum value of frequency deviation	Rad/s	-75

Parameter	Description	Units	Default Value
ω_{drp}	Frequency droop percent	pu active power/hz	0.033
Q_{drp}	Voltage droop percent	pu reactive power / pu voltage	0.045
T_r	Transducer time constant	s	0.005
T_e	Output state time constant	s	0.01
M_f	VSM inertia constant	-	0.15
d_d	VSM damping factor	-	0.11
K_{Ppll}	PLL proportional gain	-	20
K_{Ipll}	PLL integral gain	-	700
K_{Pi}	Current controller proportional gain	-	0.5
K_{Ii}	Current controller integral gain	-	20
K_{Pv}	Voltage control proportional gain	-	0.5 (if $\omega_{flag} = 0$) 3 (if $\omega_{flag} \neq 0$)
K_{Iv}	Voltage control integral gain	-	150 (if $\omega_{flag} = 0$) 10 (if $\omega_{flag} \neq 0$)
K_{Pp}	Active power proportional gain	-	0.5
K_{Ip}	Active power integral gain	-	20

The objective of this work is to check if the behavior observed from this particular GFM model with a particular set of control parameters violates the IEEE Std 1547TM-2018 requirements when the model represents a DER, and whether it violates the IEEE Std 2800TM-2022 requirements when the model represents an IBR. These control parameters have been set with an initial base tuning mechanism. It is important to note that this work does not tune the behavior of the GFM model to check whether it can meet a prespecified test criteria. Therefore, the evaluation metrics considered in the tests that are described subsequently are not the pass/fail criteria for compliance. Further, the objective of this work is not to determine pros and cons of each particular type of GFM. Rather, it is to observe whether the four types of GFM control have similarities in performance. To the best extent possible, common parameters such as droop percentage and voltage and control gains have been kept the same across all four types of possible grid forming methods.

Also, it should be noted that the set of tests described in this document are by no means the complete set of verification tests that could be carried out to ascertain whether the GFM behavior meets the requirements of the corresponding standard.

Finally, this work does not (yet) include additional tests for GFM performance requirements that are currently not included in any of the two standards. The gap analysis of IEEE 1547 and IEEE 2800 continues to identify requirements that may be required for reliable and safe operation of GFM technology in both grid-connected and islanded mode.

The test results shown in this document are plotted using generator sign convention, which is opposite to load sign convention. In generator sign convention, a positive sequence IBR current lagging positive sequence voltage provides/injects reactive power to the system (positive reactive power); a positive sequence IBR current leading positive sequence voltage consumes/absorbs reactive power from the system (negative reactive power).

IEEE 1547-2018 Tests

Volt-Var test

This test is used to compare the performance of the generic GFM model with section 5.3.3 of IEEE Std 1547TM-2018. The section lays out requirements for the DER response following a change in the voltage magnitude at its reference point of applicability (RPA), when the DER is working at volt-var control mode.

Test criteria

The evaluation metrics that are of interest are the open loop response time and the steady state operating characteristics following a step change in the RPA voltage. The response is characterized as “open loop” if the RPA voltage is not affected by power injection of the DER.

The open loop response time in the context of volt-var function test is the time between the step change in the RPA voltage and when the reactive power output (also measured at the RPA) of the system reaches 90 % of the final steady state value, before any overshoot. The steady state value is the value the output reactive power settles to after a step change in the RPA voltage.

The baseline to measure these metrics for volt-var function are given by IEEE Std 1547TM-2018 as shown in Figure 2 and Table 2. In this work, we check if the open loop response times and steady state values obtained from the response of the GFM model are within the ranges defined in Table 2. To make a visual comparison on how the responses of the GFM model are inside or outside the ranges allowed in Table 2, the responses are plotted together with the response of a DER that is compliant with IEEE Std 1547TM-2018.

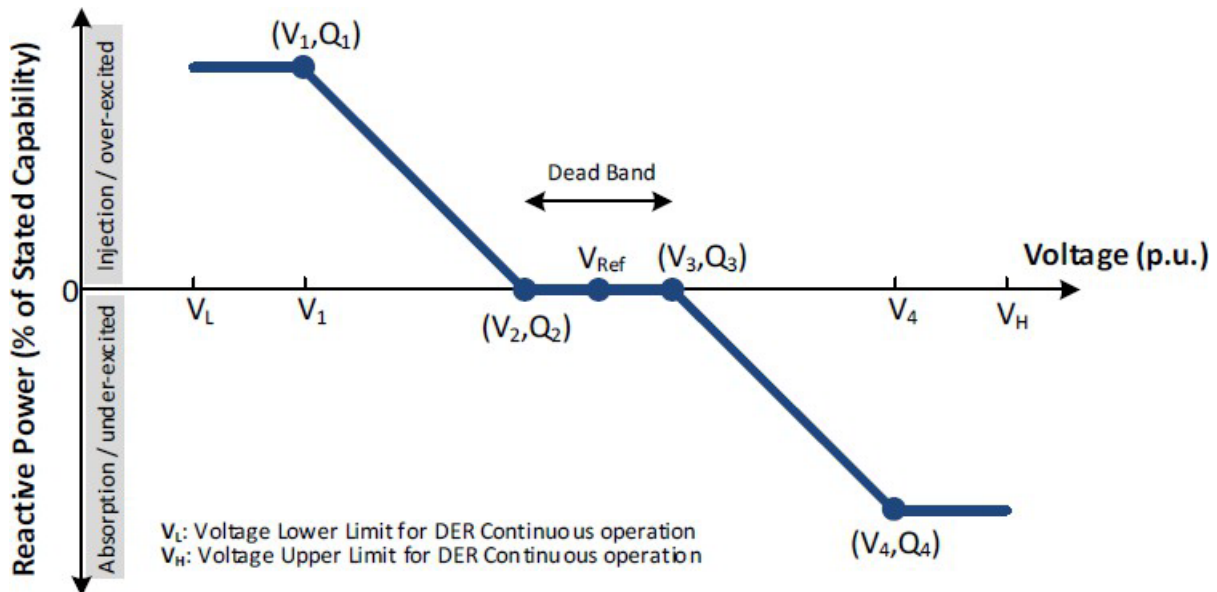


Figure 2. Volt-Var droop as per IEEE Std 1547TM-2018

Table 2. IEEE Std 1547TM-2018 voltage-reactive power settings for normal operating performance Category A and Category B DER

Voltage-reactive power parameters	Default settings		Range of allowable settings	
	Category A	Category B	Minimum	Maximum
V_{Ref}	V_N	V_N	$0.95V_N$	$1.05V_N$
V_2	V_N	$V_{Ref}-0.02V_N$	Category A: V_{Ref} Category B: $V_{Ref} - 0.03V_N$	V_{Ref}
Q_2	0	0	100% of nameplate reactive power capability, absorption	100% of nameplate reactive power capability, injection
V_3	V_N	$V_{Ref} + 0.02 V_N$	V_{Ref}	Category A: V_{Ref} Category B: $V_{Ref} + 0.03 V_N$
Q_3	0	0	100% of nameplate reactive power capability, absorption	100% of nameplate reactive power capability, injection
V_1	$0.9V_N$	$V_{Ref} - 0.08V_N$	$V_{Ref} - 0.18 V_N$	$V_2 - 0.02 V_N$
Q_1	25% of nameplate apparent power rating, injection	44% of nameplate apparent power rating, injection	0	100% of nameplate reactive power capability, injection
V_4	$1.1V_N$	$V_{Ref} + 0.08V_N$	$V_3 + 0.02V_N$	$V_{Ref} + 0.18 V_N$
Q_4	25% of nameplate apparent power rating, absorption	44% of nameplate apparent power rating, absorption	100% of nameplate reactive power capability, absorption	0
Open loop response time	10 s	5 s	1 s	90 s

Test system

Figure 3 and Figure 4 show the block diagram of the test system for this test. The generic GFM plant (including the GFM inverter, collector PI section, and step-up transformers), and the GFL

plant (including the GFL inverter and interconnection transformer) are each connected to an infinite bus. The infinite bus has a negligible impedance $r = 0.001$ ohm. Although the PSCAD library has the ideal *AC source*, the frequency and voltage settings of this component can't be changed in real time which is required for the tests performed. Therefore, a variable *AC source* with negligible impedance was used in both the GFM and the GFL test systems. It should be noted that the results presented in this report are from the measurements taken at the PCC, which is the RPA for both the GFM and the GFL plants. The feedback signals for the GFM inverter's controller are taken from the point at which the capacitor of the LCL filter is connected at the inverter terminals.

Note again the purpose of the GFL test system is to better visualize the response defined in IEEE Std 1547™-2018. It is not to compare the capability of GFL inverter with GFM inverter.

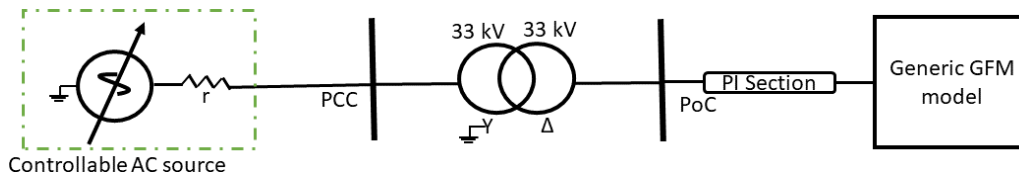
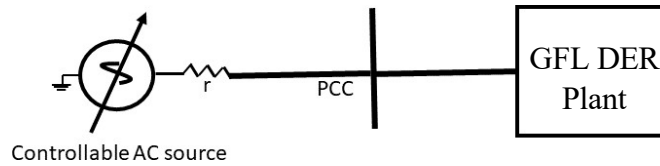


Figure 3. Test system for generic GFM model



*Interconnection transformer inside the GFL plant model

Figure 4. Test system for GFL inverter

Test results

Test platforms representing the test systems in Figure 3 and Figure 4 have been created in PSCAD. It should be noted that some modifications have to be made on the original generic GFM model. These modifications are listed below:

- The frequency droop gain is changed to 20 (5%) as oscillations in active power were observed with the default values during frequency disturbances.
- For all GFM control types except SRF-PLL, tuning of the P and Q limiters was carried out.

Step change in voltage within continuous operation region

A test case which simulates a step decrease in voltage magnitude of the *AC source* (at the RPA) within continuous operation region is setup. Table 3 and Table 4 show the configuration for the GFM model test system and GFL test system. The active power, reactive power and voltage setpoints for the GFM controller are represented as P_{pu} , Q_{pu} and V_{pu} respectively.

It can be noticed that the settings for GFL volt-var control are different from the default settings mentioned in Table 2. Especially, the open loop response time is set to the lowest value allowed

in IEEE Std 1547TM-2018. The responses of the generic GFM model and GFL model for a step change in the RPA voltage are shown in Figure 5. The responses of the GFM controls are faster compared to the response of the IEEE Std 1547TM-2018 compliant GFL inverter. The open loop response time of the GFM controls is less than 1 second (fastest response allowed in IEEE Std 1547TM-2018). Therefore, it is outside the IEEE Std 1547TM-2018 allowable range.

Table 3. Configuration for GFM test system to test volt-var clause

Parameter	Value
Ppu	0.45
Qpu	0
Vpu	1
PQ flag	1 (i.e. Q priority)
Qmax	1
Qmin	-1

Table 4. Configuration for GFL test system to test volt-var clause

Parameter	Value (pu)
V1	0.92
V2	0.98
V3	1.02
V4	1.08
Q1	0.36
Q2	0
Q3	0
Q4	-0.36
Open Loop Response Time (OLRT)	1 s

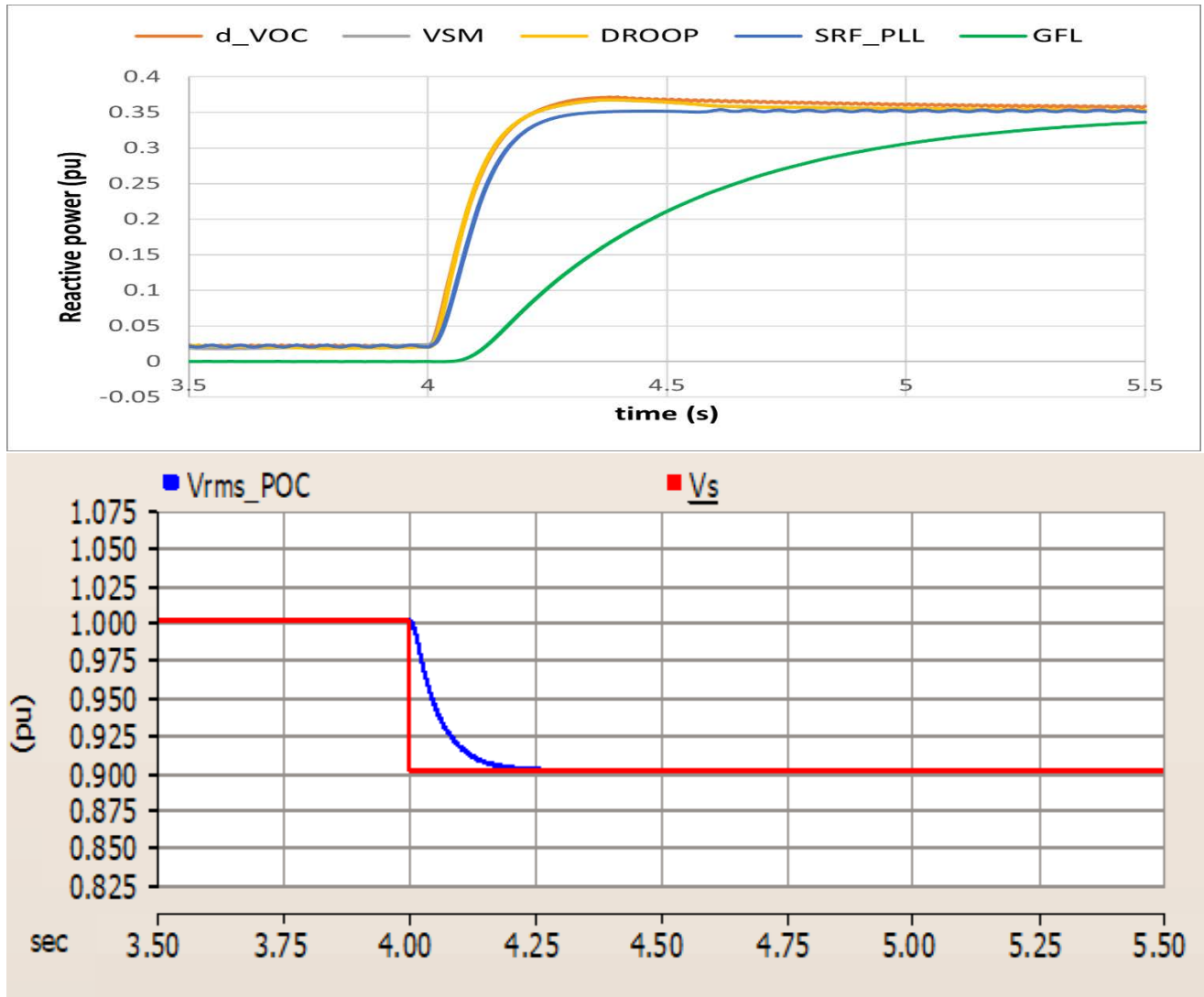


Figure 5. Response of generic GFM model and GFL inverter for a step change in AC source voltage within continuous operation region

Table 5. Open loop response time of different controllers

Controller	Open loop response time (s)
SRF PLL	0.296
Droop	0.290
VSM	0.290
d_VOC	0.290
1547 compliant GFL	1

Voltage step change in mandatory operation region

A test case in which the voltage magnitude of the RPA voltage drops to 0.8 p.u. in mandatory operation region is set up. The settings for GFM model test system are identical to the test case

of continuous operation region. For the GFL test system, the configuration is as shown in Table 6.

Table 6. Configuration for GFL inverter test system for volt-var test

Parameter	Value (pu)
V1	0.82
V2	0.97
V3	1.03
V4	1.18
Q1	0.6
Q2	0
Q3	0
Q4	-0.6
Open Loop Response Time (OLRT)	1

The responses of the generic GFM model and GFL model are shown in Figure 6. The responses of the GFM controls are faster compared to the response of the IEEE Std 1547TM-2018 compliant GFL inverter. The open loop response times of the GFM controls are shown in Table 7 and they are less than 1 second (fastest response allowed in IEEE Std 1547TM-2018 for volt-var control). However, since the RPA voltage drops into the mandatory ride-through region, IEEE Std 1547TM-2018 allows dynamic voltage support which may inject reactive current/power in a fast manner. Therefore, the GFM model behavior in this test condition may not be considered as a violation to IEEE Std 1547TM-2018. Note that IEEE Std 1547TM-2018 defines dynamic voltage support as an optional function and does not specify its performance requirements.

Furthermore, a test was run to check if the generic GFM model is effective in limiting the output reactive power within the set threshold and whether the steady state characteristics are allowed by IEEE Std 1547TM-2018. The configuration for this test is provided in Table 8. Figure 7 shows the volt-var result curve for measurements taken at inverter's terminal and the RPA (PCC). Since the inverter control takes the measurements from inverter's terminal, the reactive power is effectively limited at the inverter's terminal than at PCC. Moreover, as can be seen, the steady state operation characteristic (volt-var curve) measured at the RPA (PCC) of the GFM plant falls within the range allowed by IEEE Std 1547TM-2018. It should be noted that since the steady state response of different GFM control modes in Figure 5 and Figure 6 are close, only the response of SRF-PLL GFM control mode was plotted with an assumption that the response of other control modes would be similar.

Table 7. Open loop response time of different controllers

Controller	Open loop response time (s)
SRF PLL	0.166
Droop	0.166
VSM	0.166
d_VOC	0.166
1547 compliant GFL	1

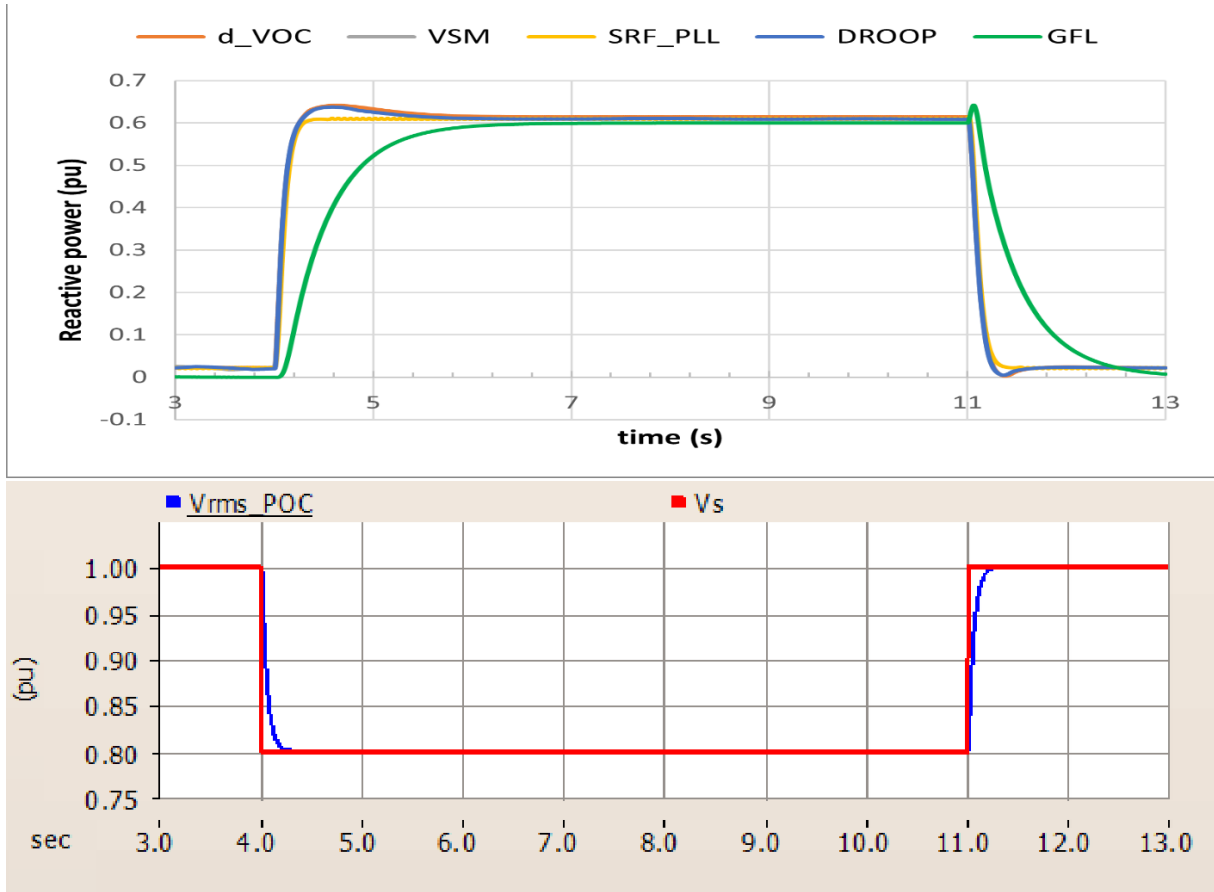


Figure 6. Response of generic GFM model and GFL inverter for a step change in AC source voltage within mandatory operation region

Table 8. Configuration for GFM test system to test volt-var curve

Parameter	Value
Ppu	1
Qpu	0
Vpu	1
PQ flag	1 (i.e. Q priority)
Qmax	0.44
Qmin	-0.44

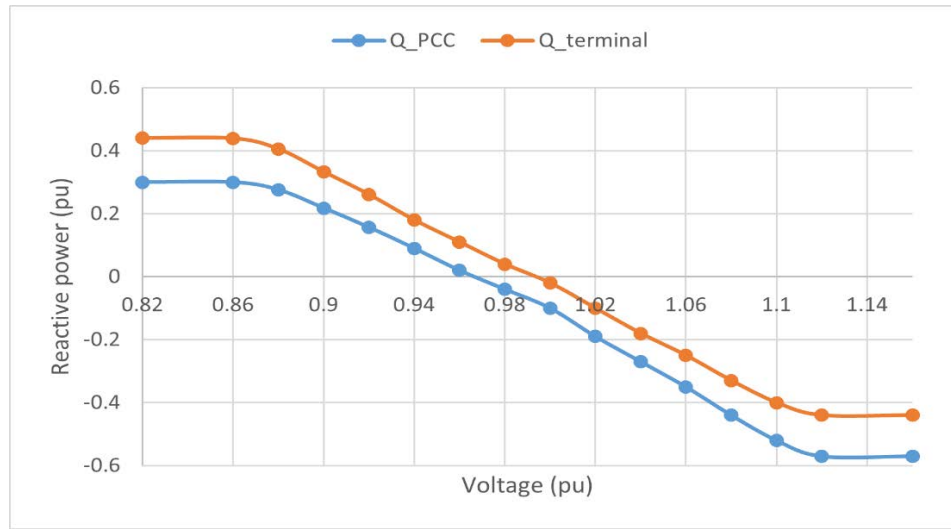


Figure 7. Volt-Var result curve for SRF-PLL GFM control mode

Frequency-droop test

This test is used to compare the performance of generic GFM model with the requirements in section 6.5.2.7 of IEEE Std 1547TM-2018. The section lays out requirements for the IBR for a change in frequency of *the grid voltage* to which it is connected.

Test criteria

The test criteria for this test are also the steady state value and the open loop response time for a step change in frequency of the *AC source*. The open loop response time in the context of frequency droop test is the time between the step change in the AC source frequency and when the active power output of the system reaches 90 % of the final steady state value, before any overshoot. The steady state value is the value the output active power settles to after a step change in the AC source frequency. The formulas that define the steady state operation characteristics of the frequency-droop function are given in (1) and (2), and the associated default parameters and allowable range are shown in Table 7b, which will be checked against.

$$P = \min_{f < 60 - db_{UF}} \left\{ P_{pre} + \frac{(60 - db_{UF}) - f}{60k_{UF}}; P_{avl} \right\} \quad (1)$$

$$P = \max_{f > 60 + db_{OF}} \left\{ P_{pre} - \frac{f - (60 + db_{OF})}{60k_{UF}}; P_{min} \right\} \quad (2)$$

where

- P : Active power output in p.u of the DER nameplate active power rating
- f : Disturbed system frequency in Hz
- P_{avl} : Available active power in p.u of the DER rating
- P_{pre} : Pre-disturbance active power output defined by the active power output at the point of time the frequency exceeds the deadband in p.u of the DER rating
- P_{min} : Minimum active power output due to DER prime mover constraints in p.u of the DER active power rating in kW
- db_{OF} : Single sided deadband value for high-frequency in Hz
- db_{UF} : Single sided deadband value for low-frequency in Hz
- k_{OF} : Per-unit frequency change corresponding to 1 per-unit power output change (frequency droop), unitless
- k_{UF} : Per-unit frequency change corresponding to 1 per unit power output change (frequency droop), unitless

The default values of these parameters are given in Table 7b.

Table 7b. Default values and allowable range of frequency droop setting

Parameter	Default Settings			Ranges of allowable settings		
	Category I	Category II	Category III	Category I	Category II	Category III
db _{OF} , db _{UF} (Hz)	0.036	0.036	0.036	0.017-1.0	0.017-1.0	0.017-1.0
k _{OF} , k _{UF}	0.05	0.05	0.05	0.03-0.05	0.03-0.05	0.02-0.05
T _{response} (s) (small signal)	5	5	5	1-10	1-10	0.2-10

Test system

The test system for this test is the same as shown in Figure 3 and Figure 4.

Test results

A test case which simulates a step change in frequency of the *AC source* connected at the PCC is created. The modifications made to the generic GFM model as described in section 2.3 are required for this test as well. The setpoints for P_{pu} , Q_{pu} and V_{pu} are 0.55, 0 and 1 respectively. For GFL, the default settings corresponding to Category III DER are applied except for OLRT which is set at 0.2 s. The response of the different control modes in generic GFM model and the response of GFL inverter are shown in Figure 8.

The open loop response times obtained for this test are given in Table 8b. It should be noted that the response of generic GFM model is faster than that of GFL model. In fact, the open loop response time is less than the minimum value of the allowable ranges for Category I, II and III DERs shown in Table 7b.

However, foot note b under Table 24 in IEEE Std 1547TM-2018 (same as Table 9 in this report) indicates that response times may be set to lower values than the minimum values shown in the table (1s for Category I and II, and 0.2s for Category III). Therefore, the response time of the GFM model to a frequency disturbance is allowed by IEEE Std 1547TM-2018.

Similarly, a test was performed to check whether the steady state operating conditions of the GFM model violates the requirement. In this test, a step increase/decrease in *AC source* frequency was applied at the PCC and the corresponding steady state active power output was noted. The steady state active power was plotted against the frequency as shown in Figure 9. Although the plot is for SRF-PLL control but since the step response of different controllers are similar as seen in Figure 8, it can be assumed that the frequency watt curves are also similar.

It can be noticed that the frequency-watt curve is a straight line with a slope slightly less than 5%, which is inside the range of allowable settings for all the three DER performance categories. Also note that foot note c under Table 24 in IEEE Std 1547TM-2018 indicates that a deadband of less than 0.017 Hz shall be permitted for all three DER performance categories. Therefore, the steady state active power frequency (P-f) operating characteristics of the GFM model is allowed by IEEE Std 1547TM-2018.

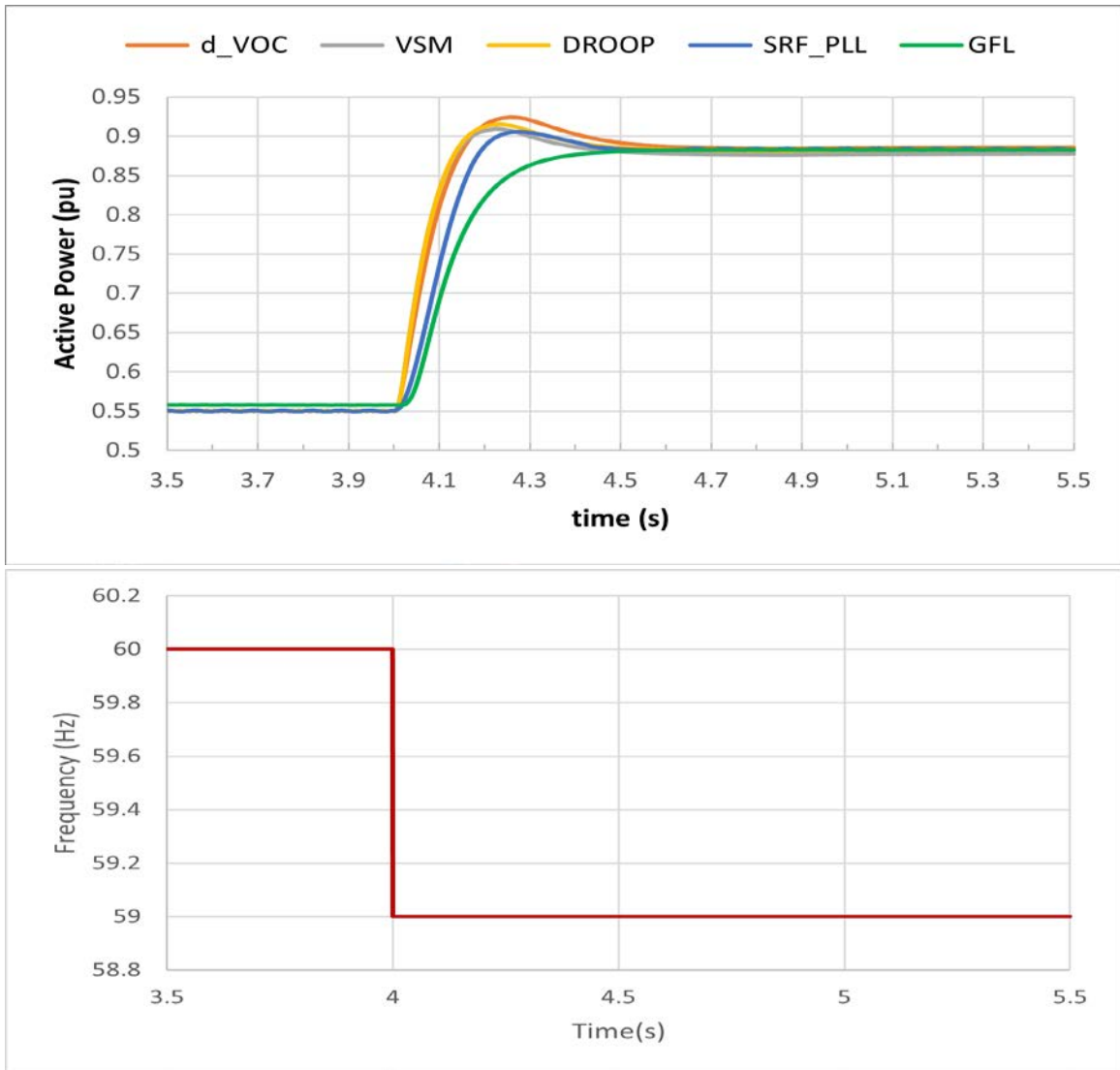


Figure 8. Response of generic GFM inverter and GFL inverter for a step change in the frequency of AC source

Table 8b. Open loop response time of different control modes

Controller	Open loop response time (s)
SRF PLL	0.12
Droop	0.08
VSM	0.08
d_VOC	0.08
1547 compliant GFL	0.2

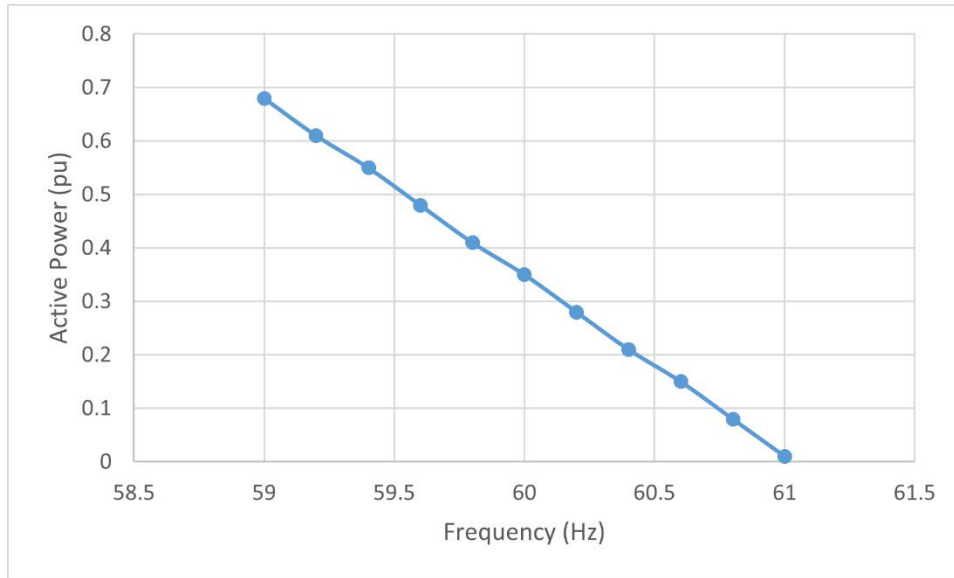


Figure 9. Frequency watt curve for SRF-PLL

IEEE 2800-2022 Tests

Reactive power-voltage control test

This test is related to the voltage control mode requirements set forth in section 5.2.2 of IEEE Std 2200™-2022. This section lays out the requirements for the dynamic reactive power response of the IBR plant to a step change in the applicable voltage within the continuous operation region. The default reference point of applicability (RPA) for this requirement is the point of measurement (POM). As per the requirement, the IBR plant shall operate in closed-loop automatic voltage control mode to regulate the steady-state voltage at the RPA to the reference value.

Test criteria

The evaluation metrics that are of interest are the reaction time, maximum step response time and damping ratio of the reactive power output response of the IBR for a step change in applicable voltage. Reaction time and step response time are defined in IEEE 2800 as:

Reaction time: “The duration from a step change in a system quantity measured at a defined location until the output of the system at the same defined location measurably changes in the direction of the control effort.”

Step response time: “The time between the step change in a system quantity measured at a defined location and when the output of the system reaches 90% of required output change, before any overshoot.”

The damping ratio is the ratio of the actual damping of the response to the damping level at the critical damping. Techniques for estimating the damping ratio based on measured data are provide in Appendix L of IEEE-2800.

The baseline to measure these matrices as mentioned in IEEE Std 2800™-2022 is given in Table 9.

Table 9. Baseline evaluation metrics for voltage-reactive power control mode as per IEEE Std 2800™-2022

Parameter	Performance target	Notes
Reaction time	<200 ms	-
Maximum step response time	As required by TS operator	Typical range: 1 s – 30 s
Damping ratio	>= 0.3	Depends on grid strength

Note: The step response characteristics will be depend on the system strength the plant is connected to.

Test system

Figure 10 shows the single line diagram of the test system. The 10 MVA generic GFM inverter is connected to a controllable AC source of short circuit ratio (SCR) of 20 through an interconnection transformer. A note here that the chosen value of SCR is an initial value of SCR.

As more evaluation tests are carried out, a variation in the value of SCR will be considered. The impedance components R_g and L_g are calculated based on the desired SCR of the source. As there is no tie-line between point of measurement (POM) and point of interconnection (POI), these two points coincide. The point of connection (PoC) is at the medium voltage (MV), 33kV side of the IBR unit transformer connected at the terminal of the inverter. Note the PoC can be either side of the IBR unit transformer in IEEE 2800-2022. The IBR unit transformer is inside the “Generic GFM model” block in Figure 10.

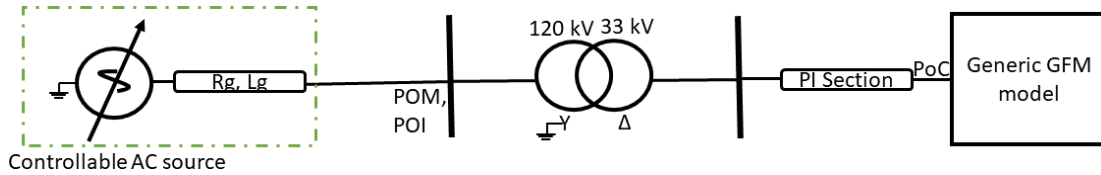


Figure 10. Test system for voltage-reactive power control test

Test results

A test platform representing the test system in Figure 10 is created in PSCAD. The tests carried out can be categorized into two types:

Step decrease in POM voltage

This test case simulates a step decrease in the magnitude of the POM voltage. The response of the generic GFM model is shown in Figure 11. The metrics indicated in IEEE 2800 are provided in Table 10. These evaluation metrics are within the allowable range.

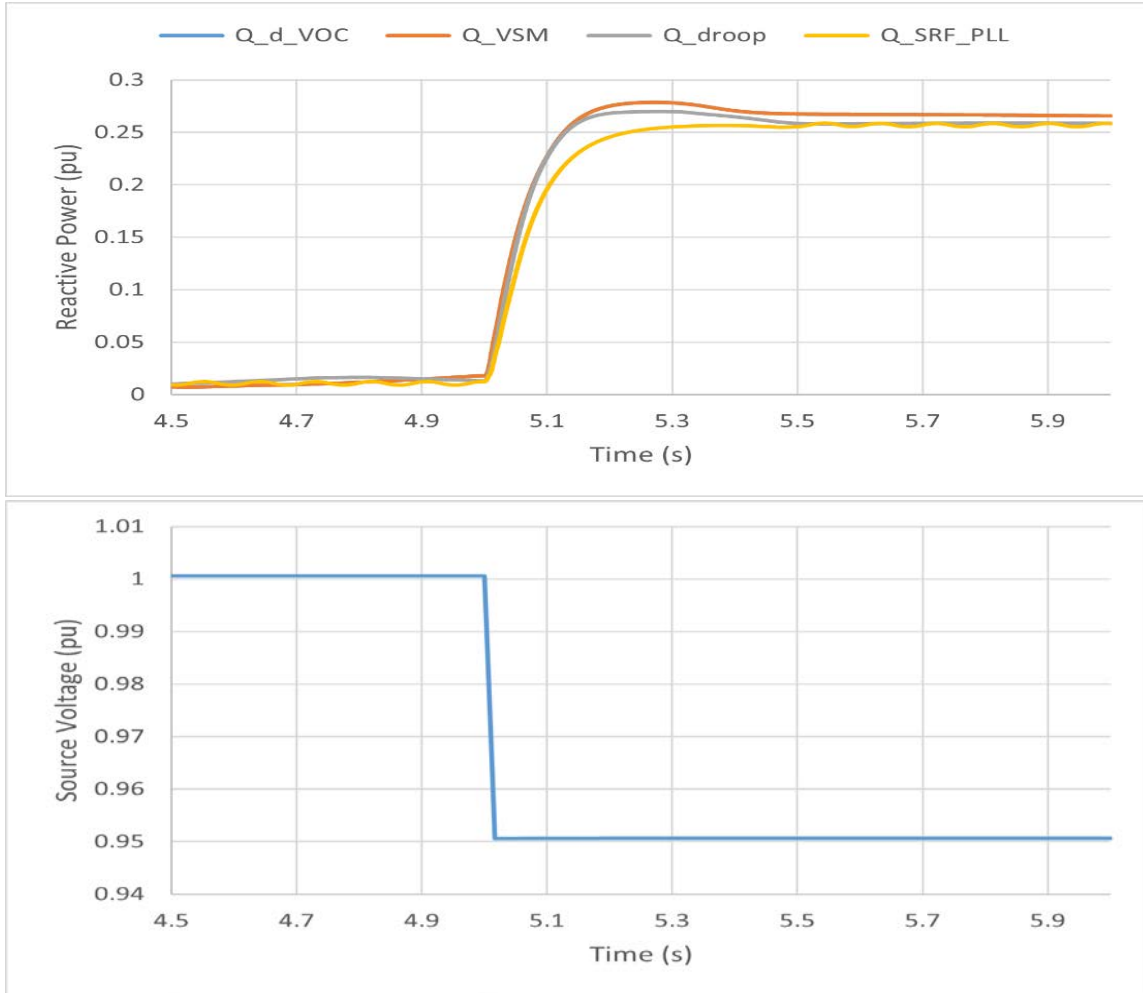


Figure 11. Generic GFM model output for a step decrease in source voltage at t = 5 s

Table 10. Values of various evaluation metrics from response of generic GFM model for a step decrease in applicable voltage

Control modes	Reaction time (ms)	Response time (s)	Damping ratio
SRF_PLL	10	0.1661	1 (critically damped)
Droop	7	0.1055	0.71
VSM	5	0.105	0.68
d_VOC	5	0.1055	0.71

Step increase in POM voltage

This test case which simulates a step increase in the magnitude of the POM voltage. The response of the generic GFM model is shown in Figure 12. The indicated in IEEE 2800 are provided in Table 11. These evaluation metrics are within the allowable range.

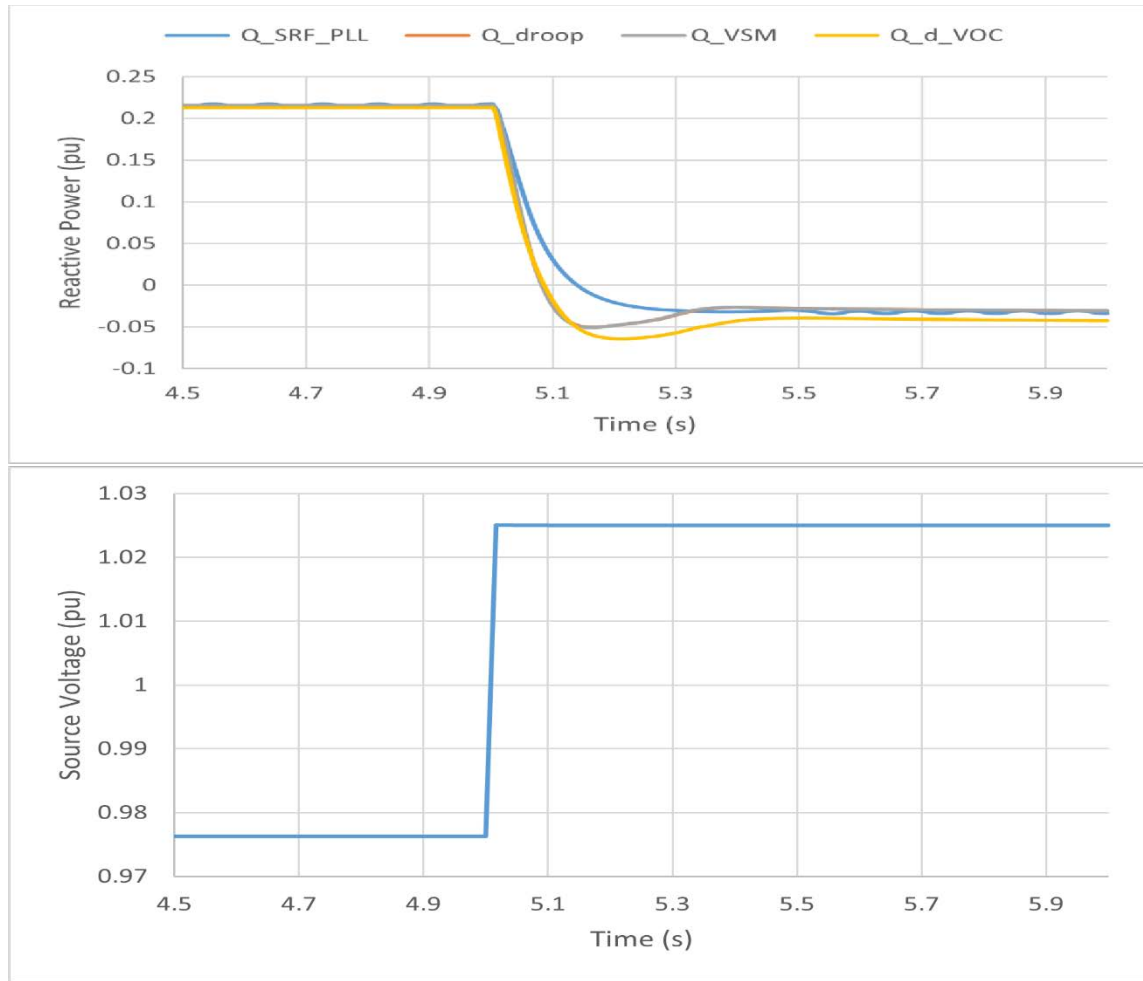


Figure 12. generic GFM model output for step decrease in source voltage at t = 5 s

Table 11. Values of various evaluation matrices for response of generic GFM model for a step decrease in applicable voltage

Control modes	Reaction time (ms)	Response time (s)	Damping ratio
SRF_PLL	11	0.08	1 (critically damped)
Droop	8	0.065	0.61
VSM	7	0.065	0.62
d_VOC	6	0.06	0.5923

Active power-frequency response test

These tests are designed to compare the performance of generic GFM model with the response requirements of an IBR to a change in system frequency as detailed in section 6 of IEEE Std 2800™-2022. The requirements related to primary frequency response (PFR) and fast frequency response (FFR1) are considered. As per the requirements, the PFR controller should have a droop function defined by (2) and (3) with parameters mentioned in Table 12.

$$p = \min \left\{ p_{avl}, p_{pre} + \max \left(0, \frac{f_{nom} - f - db_{UF}}{f_{nom} \times k_{UF}} \right) \right\} \quad (2)$$

$$p = \max \left\{ p_{min}, p_{pre} + \min \left(0, \frac{f_{nom} - f + db_{UF}}{f_{nom} \times k_{OF}} \right) \right\} \quad (3)$$

where

- p : Active power output in p.u of the IBR continuous rating (ICR)
- f : Applicable frequency in Hz
- P_{avl} : Available active power in p.u of the ICR
- P_{pre} : Pre-disturbance active power output defined by the active power output at the point of time the frequency exceeds the deadband, in the same units as p
- P_{min} : Minimum active power output due to IBR plant in p.u of the ICR
- db_{OF} : Single sided deadband value for high-frequency in Hz
- db_{UF} : Single sided deadband value for low-frequency in Hz
- k_{OF} : Per-unit frequency change corresponding to 1 per-unit power output change (frequency droop), unitless
- k_{UF} : Per-unit frequency change corresponding to 1 per unit power output change (frequency droop), unitless

Table 12. Parameters for PFR requirements

Parameter	Units	Default value	Ranges of available settings	
			Minimum	Maximum
db_{UF}	Hz	$0.06\% \times f_{nom}$	$0.025\% \times f_{nom}$	$1.6\% \times f_{nom}$
db_{OF}	Hz	$0.06\% \times f_{nom}$	$0.025\% \times f_{nom}$	$1.6\% \times f_{nom}$
k_{uf}		5%	2%	5%
KOF		5%	2%	5%

IEEE Std 2800TM-2022 also requires FFR during the arresting period of the frequency excursion. Mathematically, FFR1 is similar to PFR but with faster response time and droop up to 1 % (i.e., provide 100 % change in power for 1% change in frequency). It should be noted that FFR1 is active only up to the point where the applicable frequency reaches its nadir.

Test criteria

The test criteria for PFR test are the reaction time, rise time, settling time and damping ratio. The reaction time in the context of PFR test is the time between the step change in the applicable frequency and when the active power output of the system starts changing in the direction of the control. The rise time is the duration between the time when active power response reaches 10 %

of the steady state value and when it reaches 90 % of the steady state value. The settling time is the duration taken by the response to settle within the allowable settling band. The damping ratio is the ratio of the actual damping of the response to the damping level at the critical damping. The damping ratio may be calculated using equation (1). The baseline metrics for evaluation are given in Table 13.

Table 13. Evaluation matrices for PFR as per IEEE 2800™-2022

Parameter	Units	Default value	Minimum	Maximum
Reaction time	Seconds	0.50	0.20	1
Rise time	Seconds	4.0	2.0	20
Settling time	Seconds	10.0	10	30
Damping ratio	Unitless	0.3	0.2	1

The evaluation criterion for FFR1 is the step response time. Step response time in the context of FFR1 test is defined as duration between the inception of the applicable frequency perturbation and the time when the active power output of the IBR reached 90 % of its steady state value. The step response time of FFR1 is required to be less than 1s.

Test system

The test system for the GFM model for this test is the same as before, i.e., Figure 10.

Test results

Decrease in system frequency

A test case which simulates a decrease in applicable frequency with rate of change of frequency (ROCOF) of 3 Hz/s is created. The response of the GFM model is shown in Figure 13 and the values of the evaluation metrics are given in Table 14. The values of evaluation metrics are within the allowable range. Furthermore, since the response time is less than 1 s, the requirement of FFR1 is also fulfilled. Similarly, the operating point after the frequency change was calculated using (2) and (3) and default parameters from Table 12 and was found to be approximately 0.81 p.u. which is very close to the operating point of the GFM model.

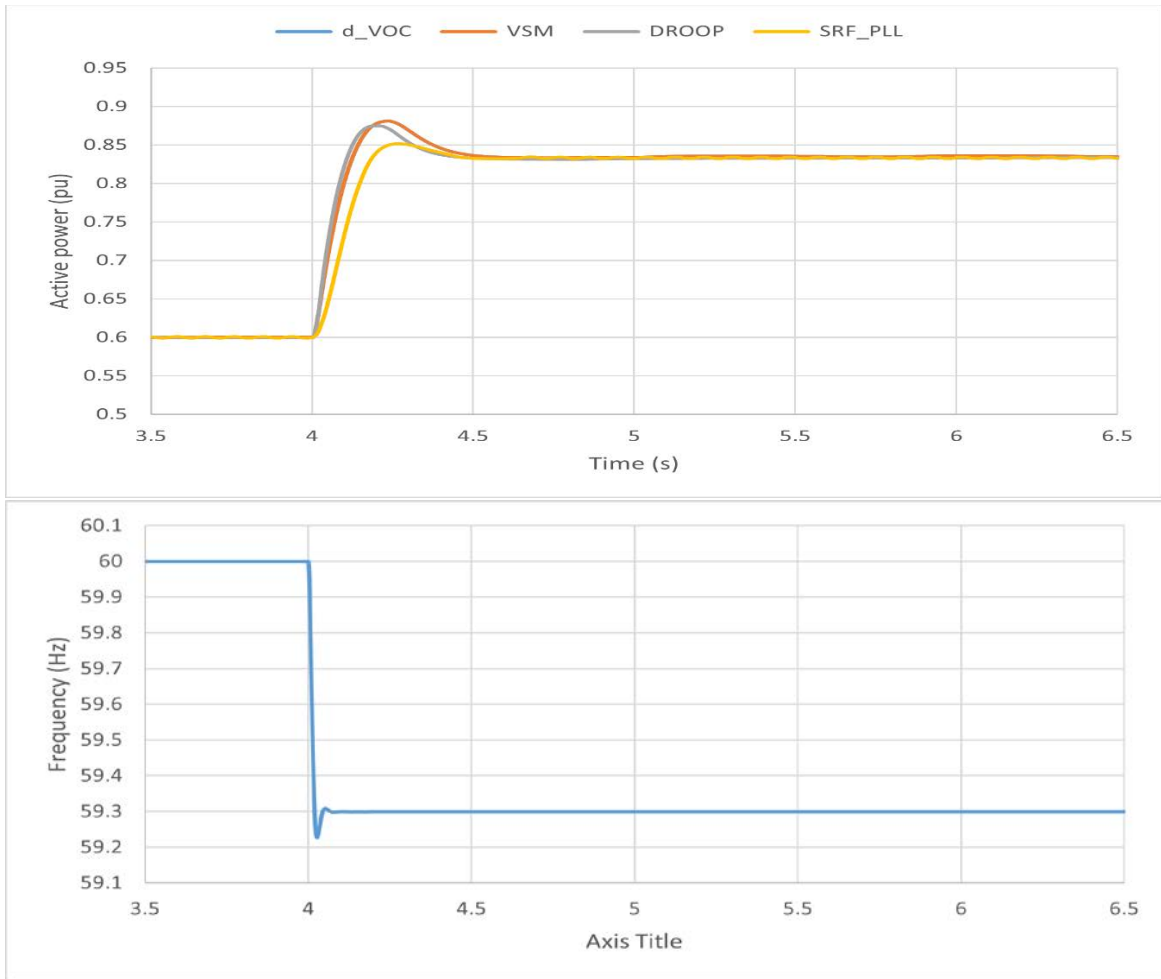


Figure 13. Response of GFM model for decrease in applicable frequency with ROCOF of 3 Hz/s

Table 14. Values of various evaluation matrices for GFM model for a decrease in applicable frequency with ROCOF of 3 Hz/s

Control mode	Reaction time (ms)	Rise time (s)	Settling time (s)	Damping ratio
SRF-PLL	11	0.139	0.48	0.6137
Droop	9	0.0756	0.49	0.514
VSM	9	0.09	0.48	0.48
d_VOC	9	0.0756	0.49	0.514

Increase in applicable frequency

A test case which simulates an increase in applicable frequency with rate of change of frequency (ROCOF) of 3 Hz/s is created. The response of the GFM model is shown in Figure 14 and the values of the evaluation metrics are given in Table 15. It can be seen that the evaluation metrics are within the allowable range. Furthermore, since the response time is less than 1 s, the

requirement of FFR1 is also fulfilled. The operating point calculated from the default parameters of PFR droop function is close to the operating point of the GFM model in this test as well.

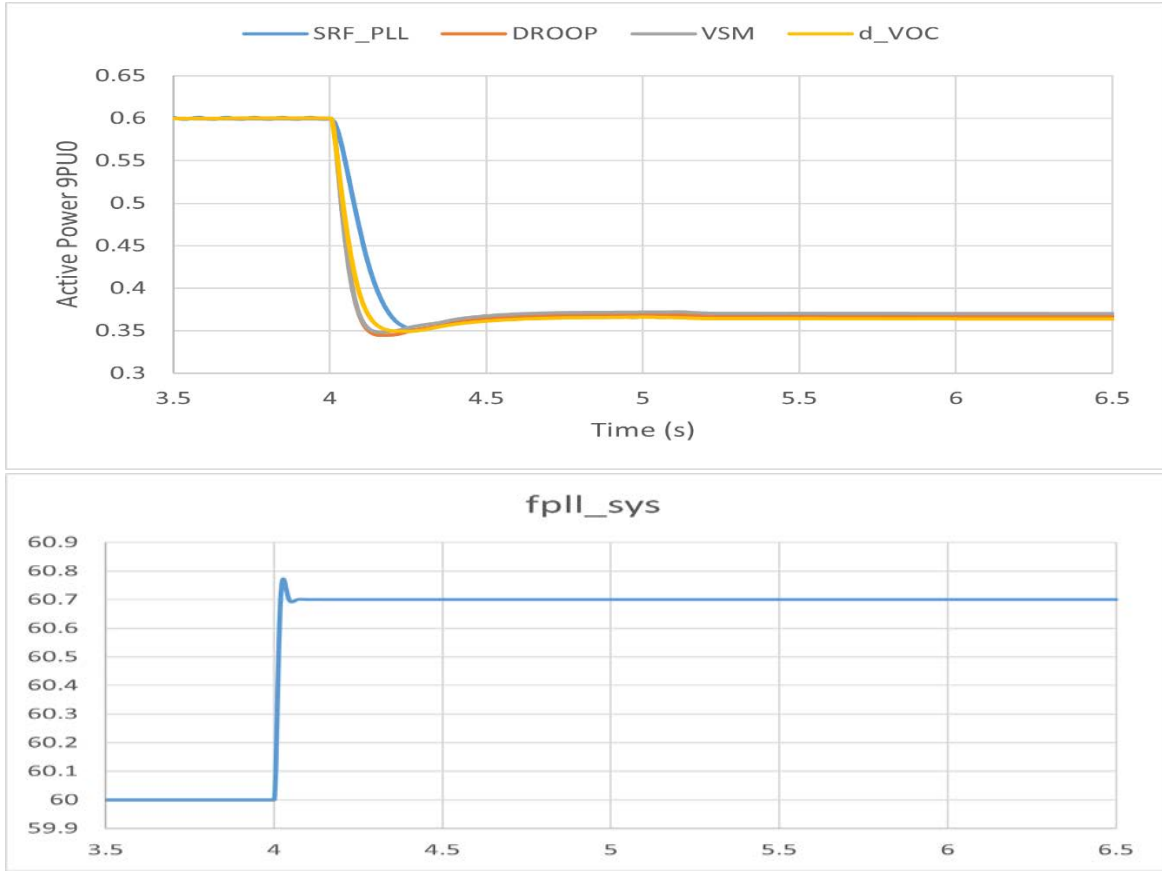


Figure 14. Response of GFM model for increase in applicable frequency with ROCOF of 3 Hz/s

Table 15. Values of various evaluation matrices for GFM model for increase in applicable frequency with ROCOF of 3 Hz/s

Control mode	Reaction time (ms)	Rise time (s)	Settling time (s)	Damping ratio
SRF-PLL	10	0.1452	0.46	1 (critical damping)
Droop	9	0.0674	0.45	0.876
VSM	9	0.0674	0.45	0.876
d_VOC	8	0.0866	0.46	0.876

Low voltage ride-through response test

This test compares the performance of the response of the generic GFM model with the low and high voltage ride-through response requirements set forth in section 7.2.2.3 of IEEE Std 2800TM-2022. This section describes the required response capability of the inverter when in the mandatory operating region defined in IEEE 2800-2022 section 7.2.2. This work has specifically

compared the performance of the GFM model with the current injection requirements specified in section 7.2.2.3.4. The default RPA for current injection during ride through mode is the POC.

Test criteria

The IEEE 2800-2022 standard does not specify the magnitude of incremental positive sequence and negative sequence reactive current. The standard requires the IBR unit to:

- Inject reactive current dependent on the IBR unit terminal voltage for balanced faults
- Inject negative sequence current dependent on the IBR unit terminal negative sequence voltage that leads the negative sequence voltage by 90-100 degrees. This is in addition to the positive sequence reactive current.

The nomenclature used in this work to indicate the different components of the current is:

- Positive sequence active current: $i_{7c} = |I_1| \cos(\angle V_1 - \angle I_1)$
- Positive sequence reactive current: $i_{7s} = |I_1| \sin(\angle V_1 - \angle I_1)$
- Negative sequence active current: $i_{9c} = |I_2| \cos(\angle V_2 - \angle I_2)$
- Negative sequence reactive current: $i_{9s} = |I_2| \sin(\angle V_2 - \angle I_2)$

The phasor domain values are calculated by a discrete Fourier transform (DFT) of one cycle of the fundamental frequency of the sampled instantaneous values. The data window is shifted through the sampled data set to get the variation of the phasor domain values as a function of time.

The response of the IBR unit is compared to the response requirements in Table 16. The time delay required for the DFT measurements is included in the step response time and settling time mentioned in Table 16.

Table 16. Performance specification for current injection during voltage ride through events

Parameter	IBR units except Type III WTGs
Step response time	≤ 2.5 cycles (0.04167 s)
Settling time	≤ 4 cycles (0.0667 s)
Settling band	-2.5 % / + 10 % of IBR unit maximum current

Test system

The test system used for this test is the same as in Figure 10. The tests are carried out at active power level of 0.8pu on the rating of the IBR. Further operating points may need to be tested in future to observe the impact of different techniques of applying current limits.

Test results

Two tests related to voltage ride through requirements are performed. They are balanced LLLG fault and unbalanced LG fault. The LG fault was chosen as it is the most commonly occurring fault on the network.

Unbalanced fault (L-G fault)

This test considers a voltage drop in phase A from 5s to 6 s of the controllable AC source consistent with a phase A to ground fault as shown in Figure 15. The responses of the GFM model are given in Figure 16- Figure 20 and the values of the performance specifications are given in Table 17.

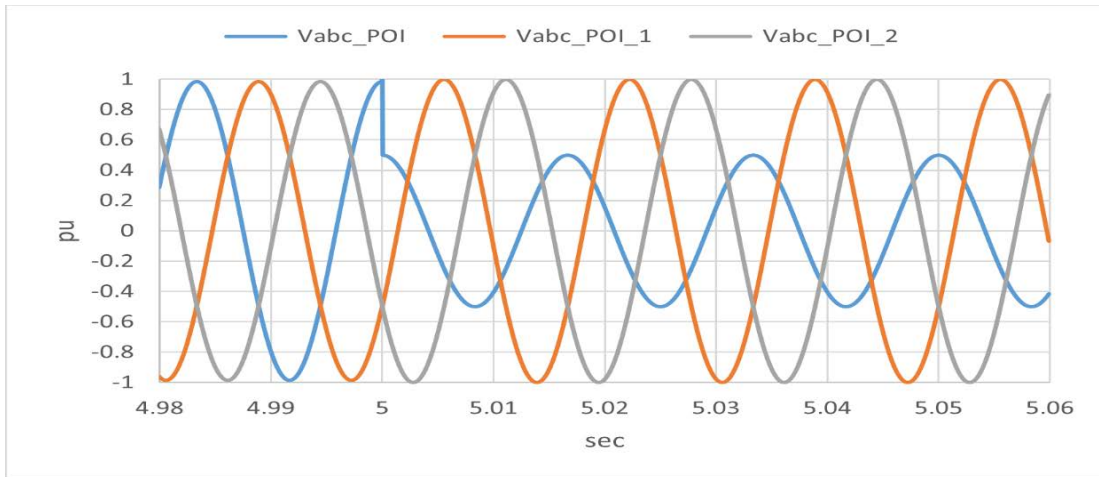


Figure 15. POC voltage during LG fault

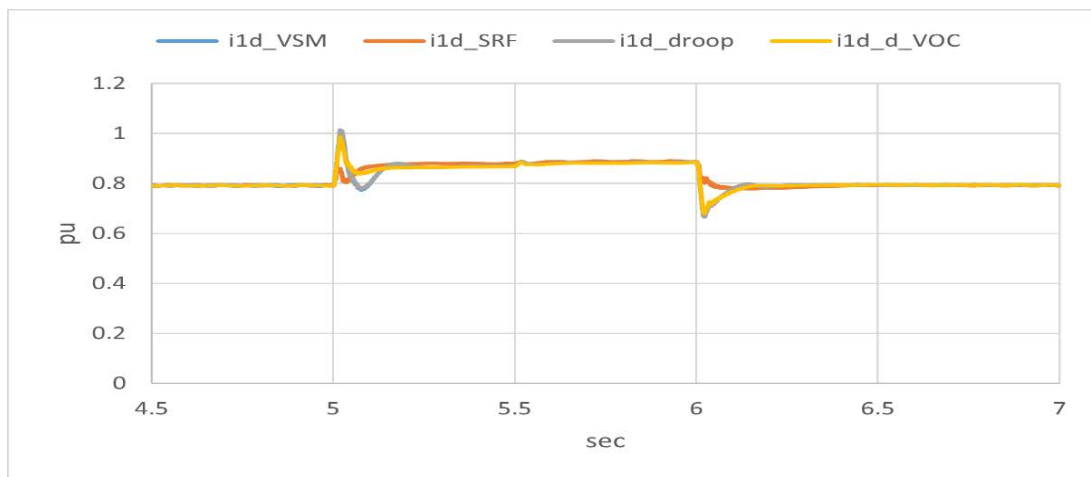


Figure 16. Positive sequence active current

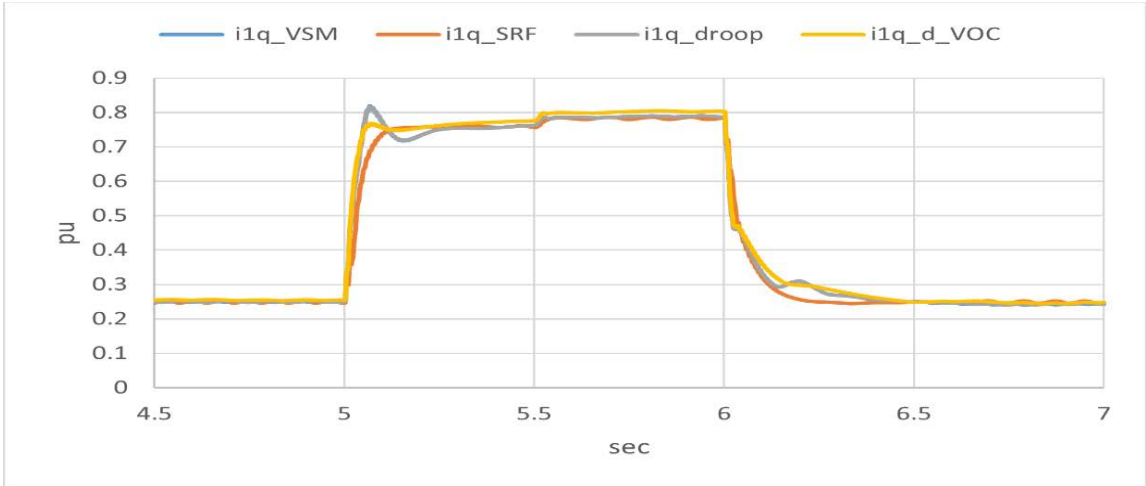


Figure 17. Positive sequence reactive current

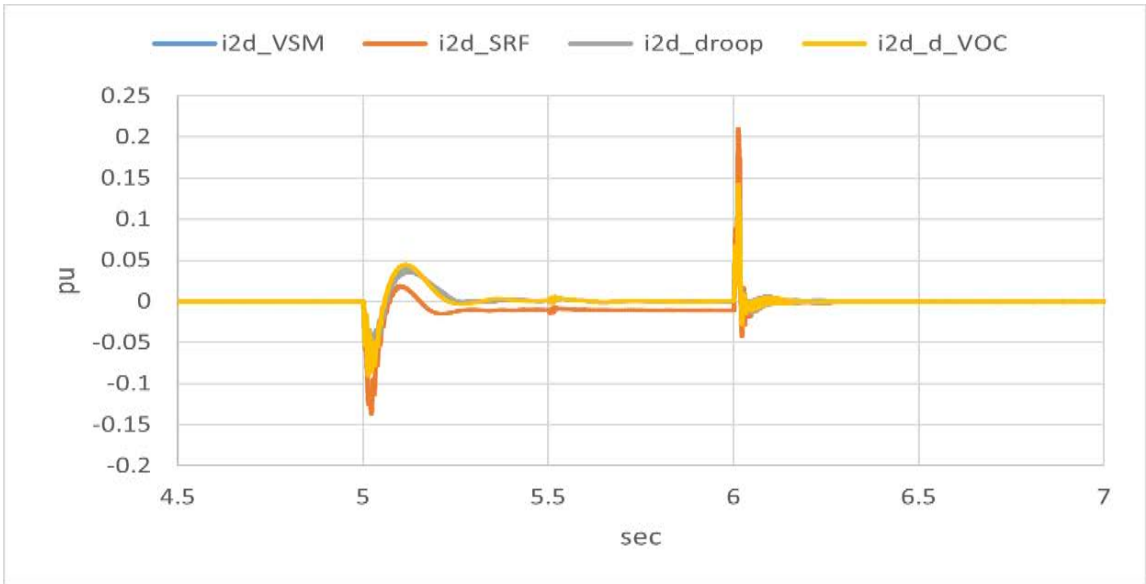


Figure 18. Negative sequence active current

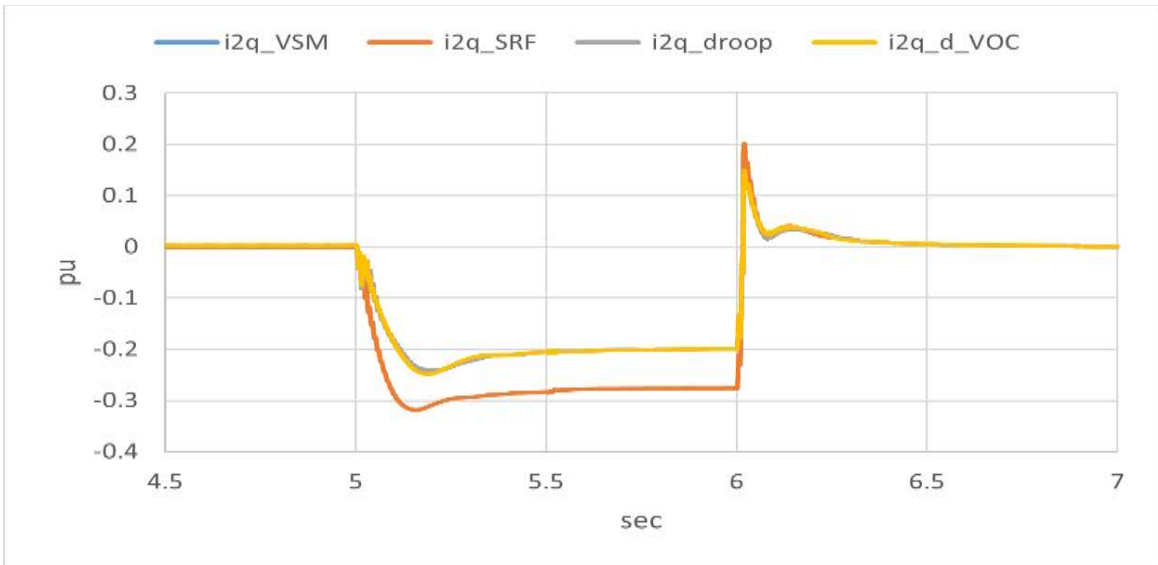


Figure 19. Negative sequence reactive current

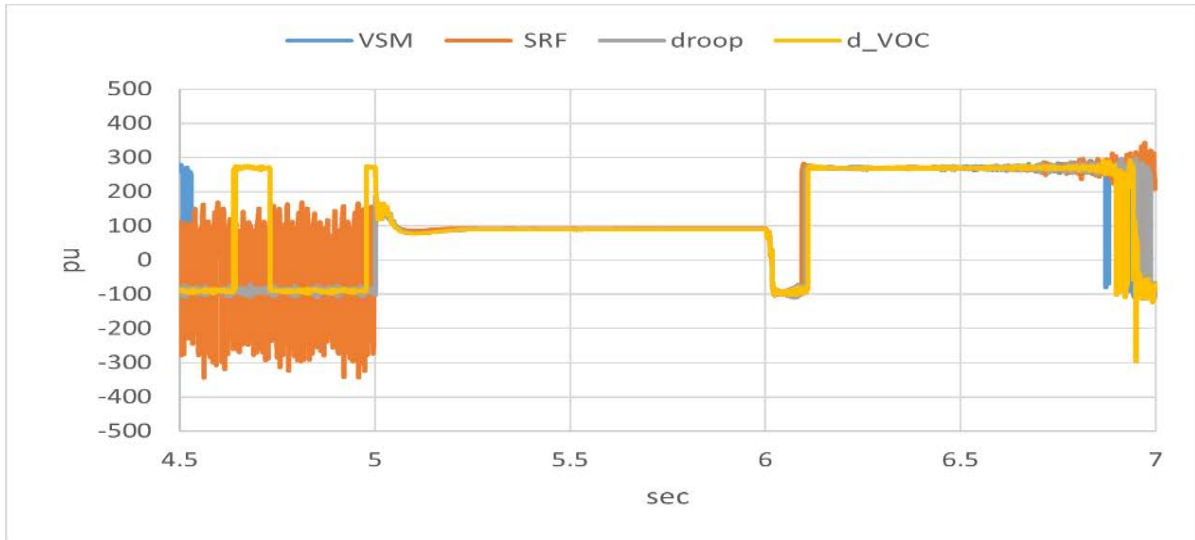


Figure 20. Phase difference between negative sequence reactive current and negative sequence voltage

Table 17. Values of evaluation metrics for LG fault

GFM control mode	Step response time			Settling time				
	Positive sequence reactive current (s)	Positive sequence active current (s)	Negative sequence reactive current (s)	Negative sequence active current (s)	Positive sequence reactive current (s)	Positive sequence active current (s)	Negative sequence reactive current (s)	Negative sequence active current (s)
SRF- PLL	0.04275	0.15	0.0782	0.07	0.1229	0.10	0.079	0.24
Droop	0.04065	0.5	0.099	0.06	0.2075	0.10105	0.08545	0.23
VSM	0.04065	0.5	0.099	0.06	0.2075	0.10105	0.08545	0.23
d_VOC	0.04065	0.5	0.099	0.06	0.2995	0.10105	0.08545	0.23

The results show that the inverter injects reactive current in both the positive and negative sequences consistent with the IEEE 2800-2022 requirements. However, the time domain response characteristic of the IBR unit shown in Table 17 do not strictly meet the time domain response requirements (specified in Table 16). It is to be discussed whether the specifications in the standard apply to all types of current.

Balanced fault (LLL fault)

This test case considers a balanced voltage drop in three phases of the controllable AC source from 5 s to 6 s consistent with a three-phase fault. The response of the GFM modes are shown in Figure 22 and Figure 23. The values of the performance specifications are tabulated in Table 18. It is observed that the positive sequence current from each type of GFM has a different response as compared to other GFM methods. The cause for this difference and whether it has an impact on the grid is to be investigated in future work.

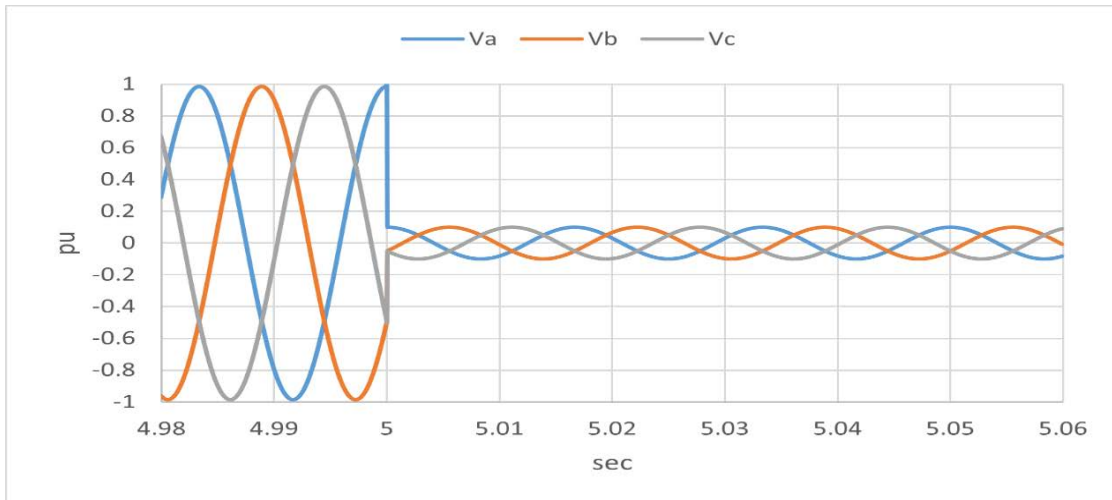


Figure 21. POC voltage for balanced LLLG fault

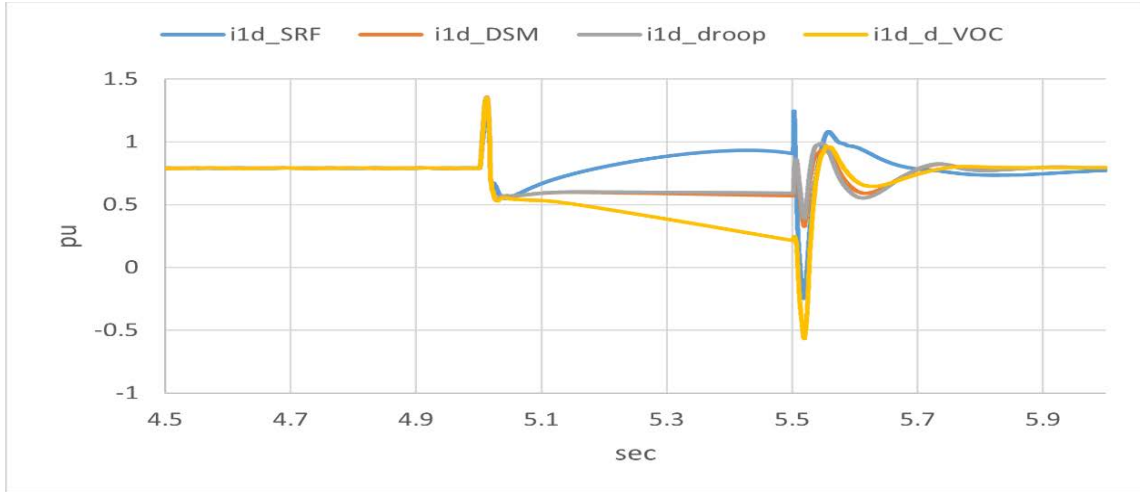


Figure 22. Positive sequence active current for balanced LLLG fault

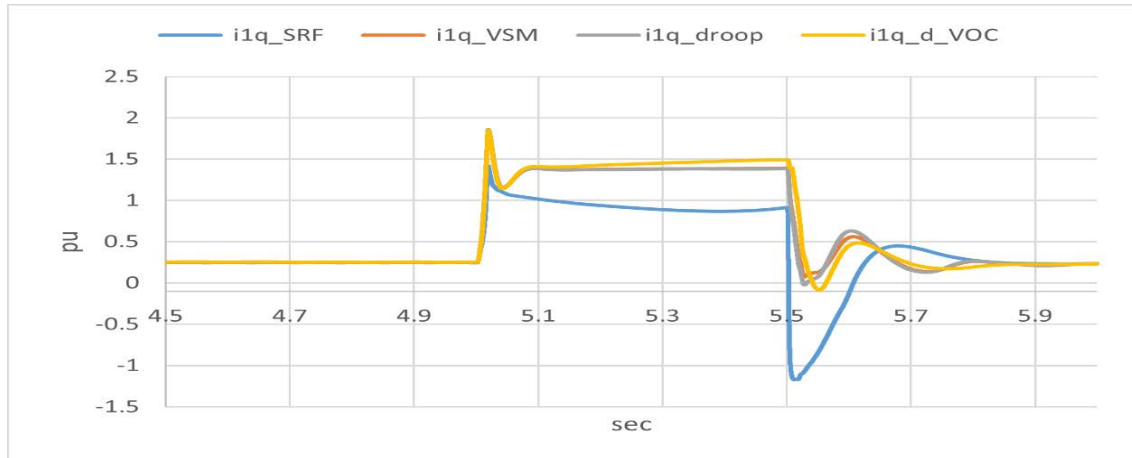


Figure 23. Positive sequence reactive current for balanced LLLG fault

Table 18. Values of performance specifications for LLLG fault

Control mode	Step response time (s)		Settling time (s)	
	Positive sequence active current	Positive sequence reactive current	Positive sequence active current	Positive sequence reactive current
SRF-PLL	0.34	0.0146	0.5	0.1
Droop	0.05	0.0146	0.05	0.1
VSM	0.05	0.0146	0.05	0.1
d_VOC	0.05	0.0146	-	0.1

Figure 23 shows that the GFM models inject reactive current in the positive sequence during the balanced fault consistent with the IEEE 2800-2022 requirements. The time domain response

characteristic of the IBR unit shown in Table 18 do not strictly meet the time domain response requirements (specified in Table 16).

Voltage phase angle change test

IEEE Std 2800™ – 2022 Clause 7.3.2.4 specifies that “the IBR plant shall ride through positive sequence phase angle changes within a sub-cycle-to-cycle time frame of the applicable voltage of less than or equal to 25 electrical degrees.” The standard requires that any current oscillations are positively damped.

Test system

The test system used for these tests is the same as Figure 10. The tests are carried out at active power levels of 0.1pu, 0.6pu and 0.9pu on the rating of the IBR.

Test results

A test case is created to simulate the different types of phase jumps.

Balanced phase jump of -30 degrees

In this test, the phase angle of the system voltage shifts by -30 degrees at $t = 5\text{s}$ and +30 degrees at $t = 6\text{s}$. Plots of instantaneous power and currents will be plotted in future versions. The active power and reactive power plots in Figure 25 - Figure 27 show that the GFM model is able to ride through such a phase jump. It can be noticed that the reactive power output is not exactly at the set point. This is because the controller is maintaining the active and reactive power output at its terminal to be equal to the set-point. Since the measurements for the plots are taken from the POM, some amount of reactive power is consumed by the interconnection transformer that is between POC and POM.

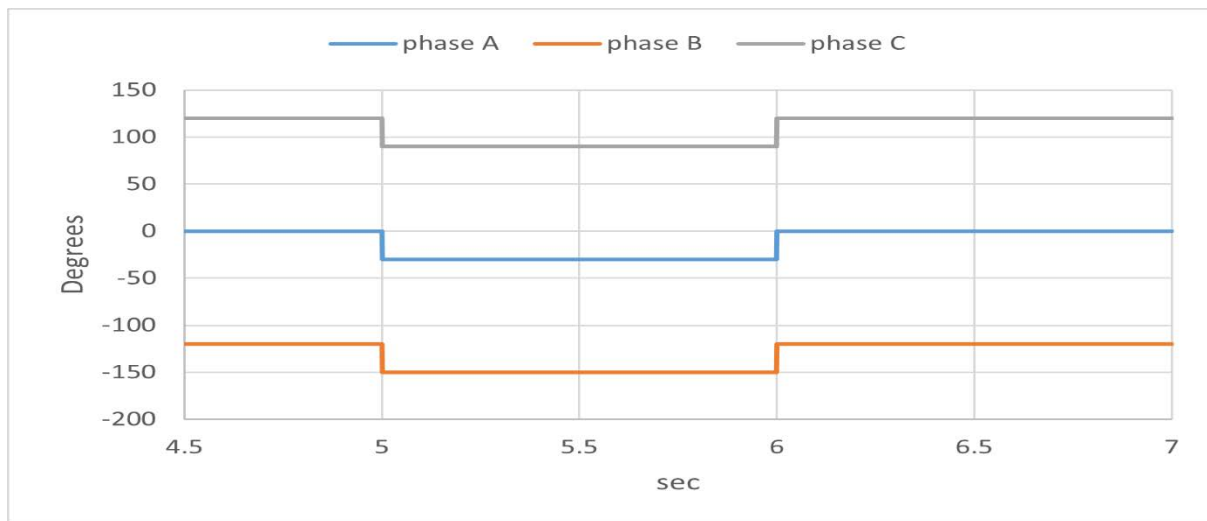


Figure 24. Balanced phase jump in POM voltage

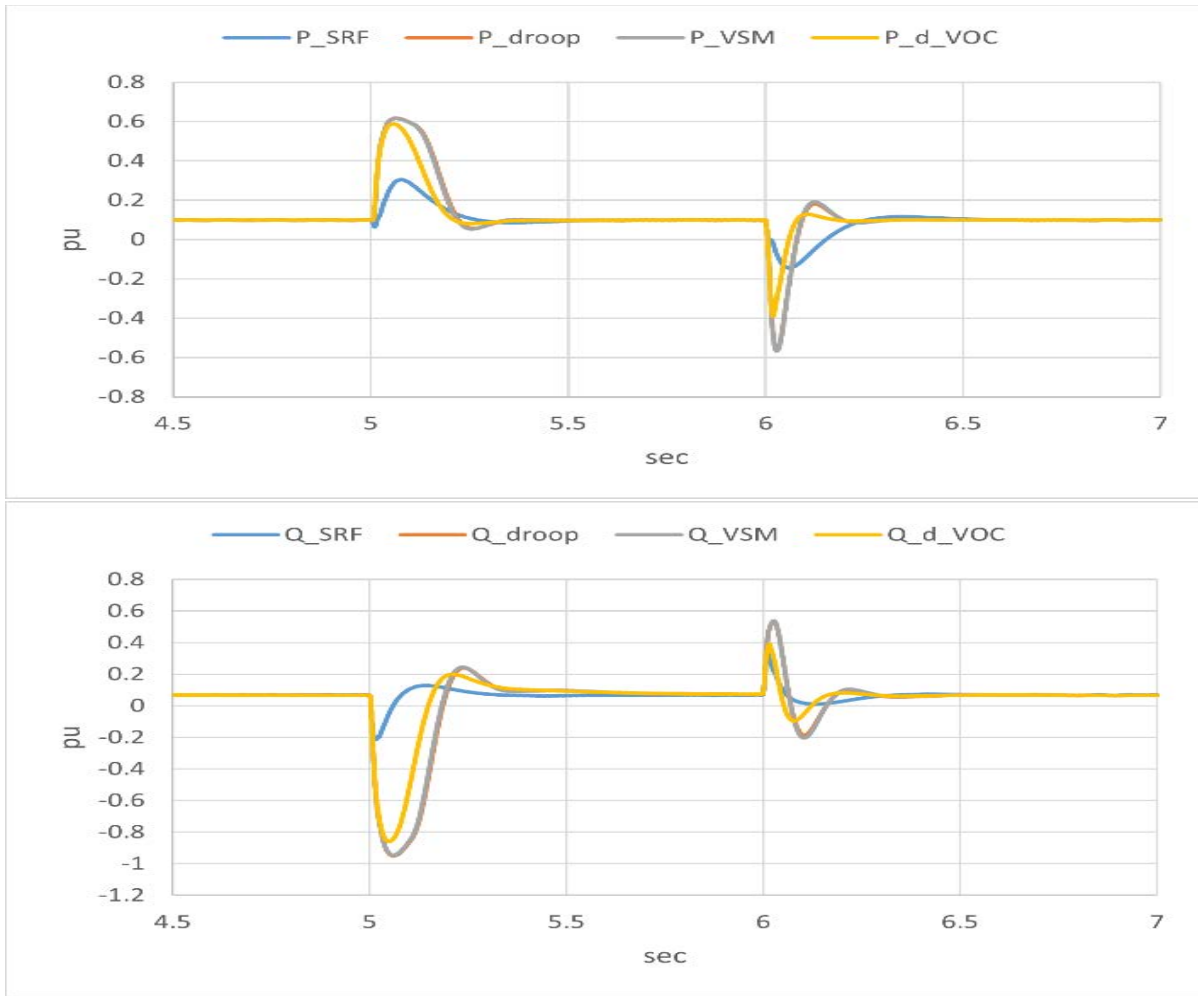


Figure 25. Response of GFM model for balanced negative phase jump when $P = 0.1$ p.u., $Q = 0.1$ p.u.

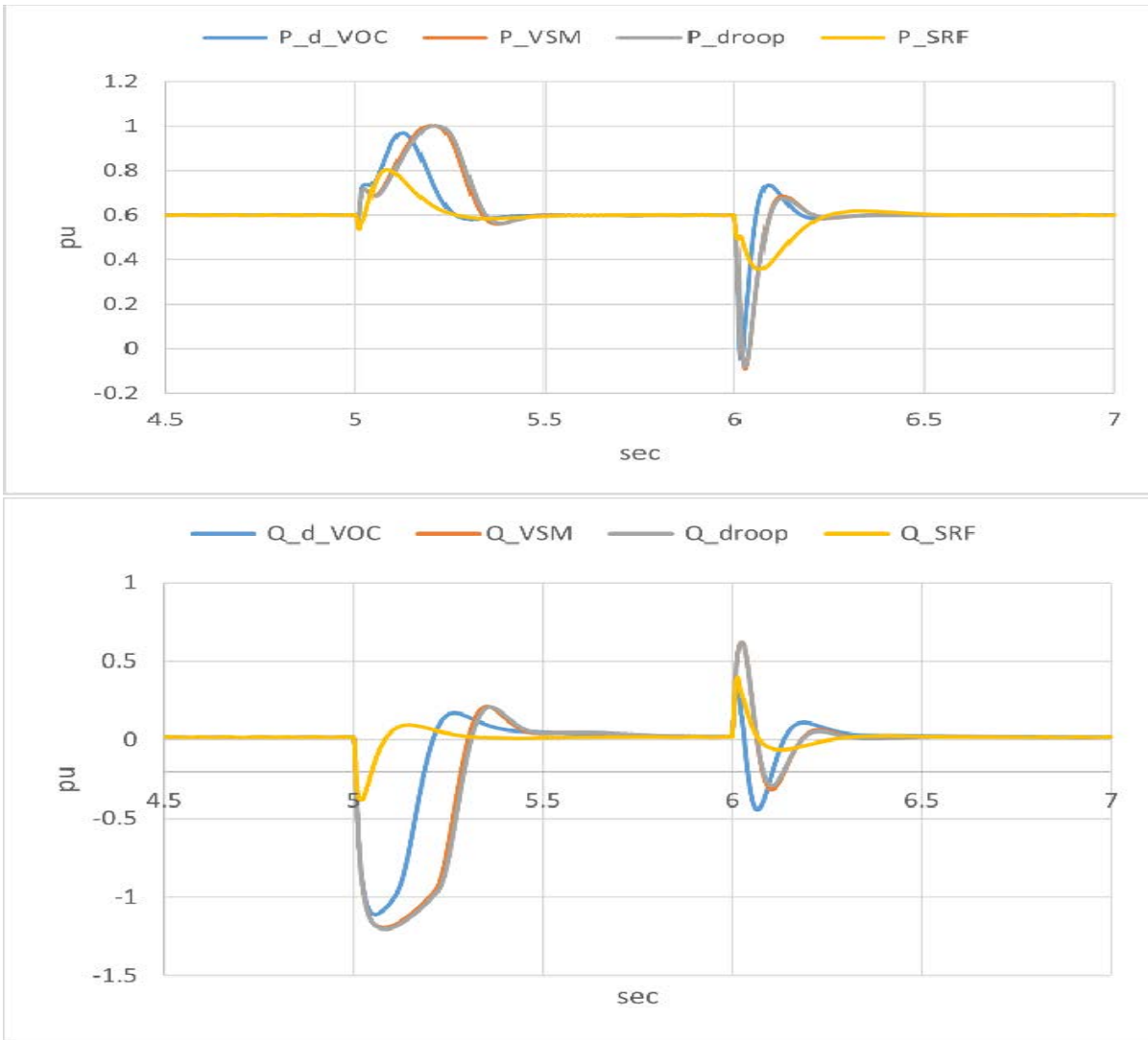


Figure 26. Response of GFM model for balanced negative phase jump when $P = 0.6$ p.u., $Q = 0.1$ p.u.

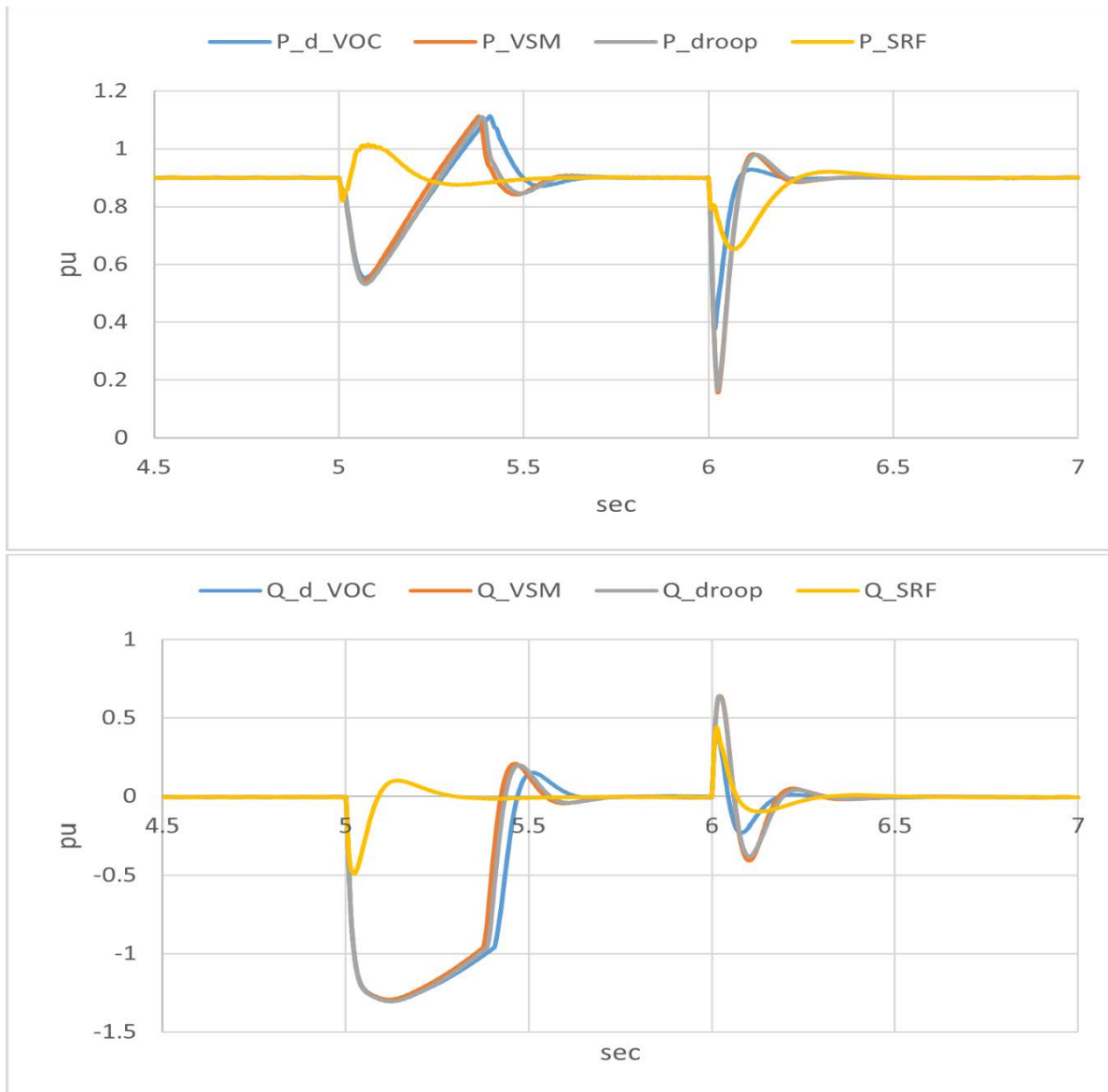


Figure 27. Response of GFM model for balanced negative phase jump when $P = 0.9$ p.u., $Q = 0.2$ p.u.

Balanced phase jump of +30 degrees

In this test, the phase angle of the system voltage shifts by +30 degrees at $t = 5$ s and -30 degrees at $t = 6$ s. The active power and reactive power plots in Figure 29 - Figure 31 show that the GFM model is able to ride through such phase jump.

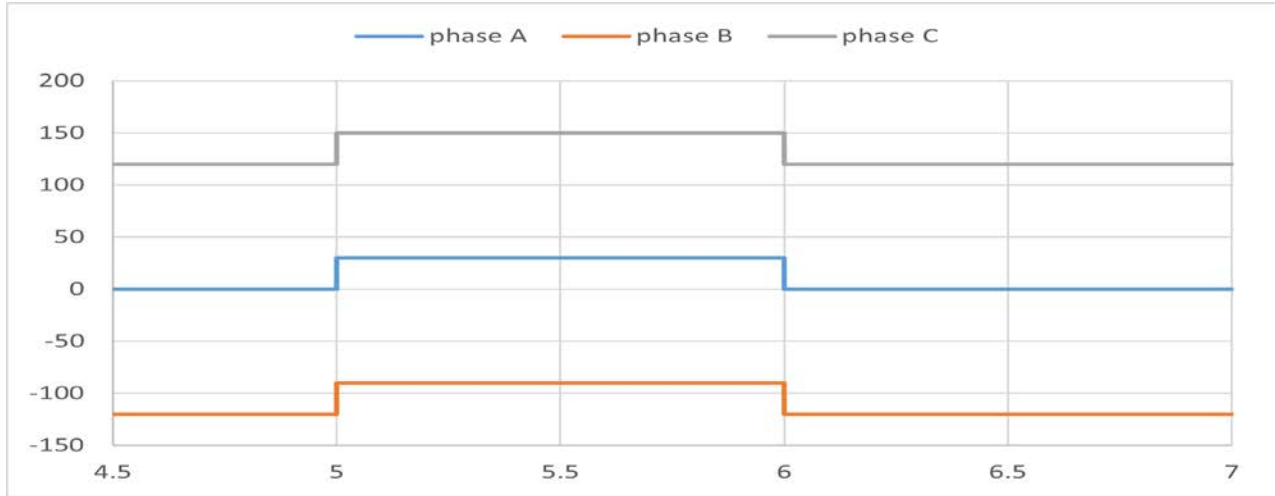


Figure 28. balanced positive phase jump in applicable voltage

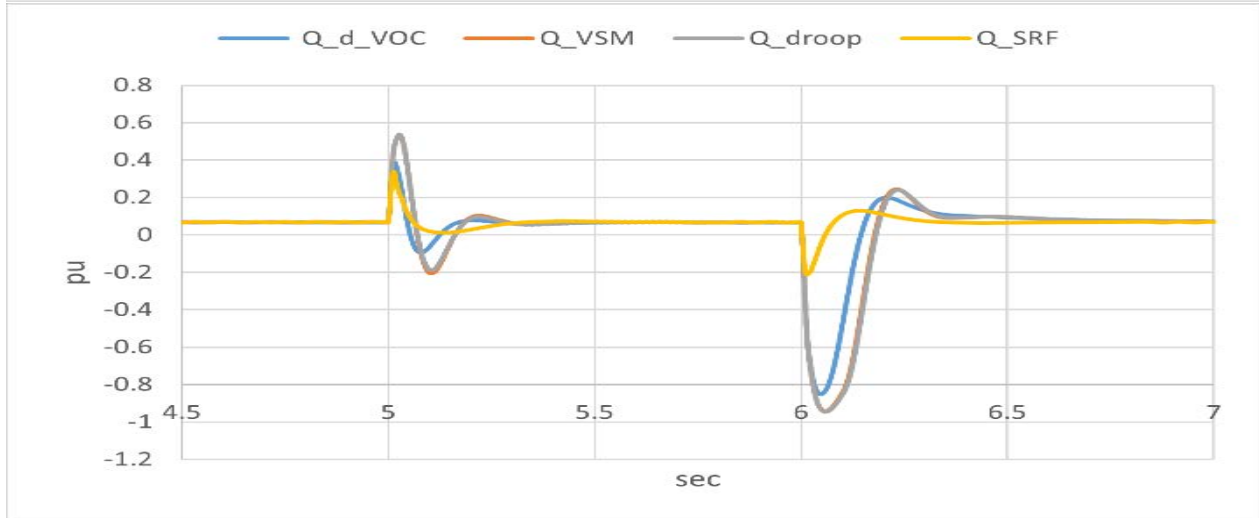
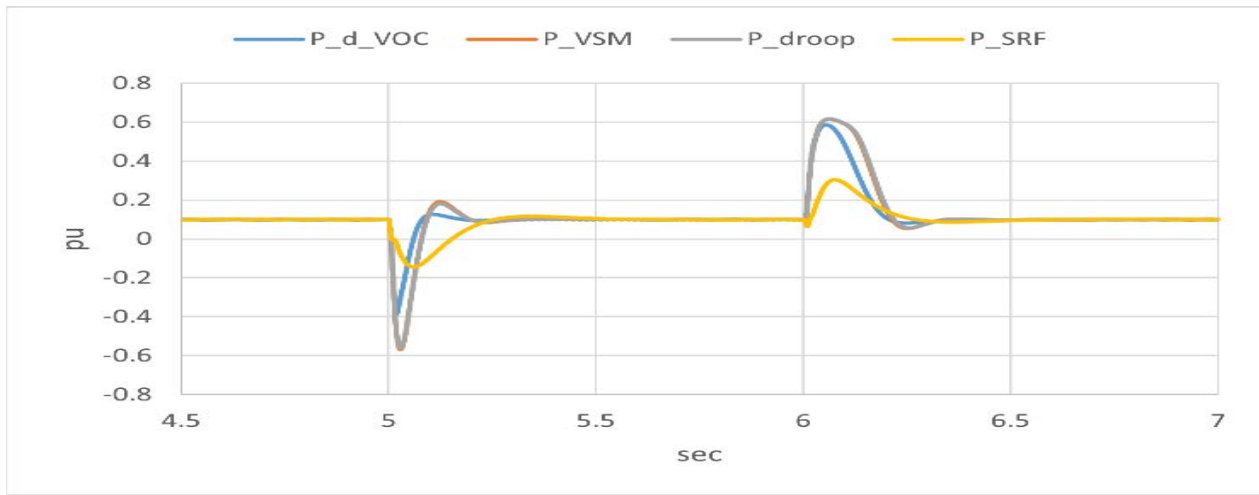


Figure 29. Response of GFM model for balanced positive phase jump when $P = 0.1$ p.u., $Q = 0.1$ p.u.

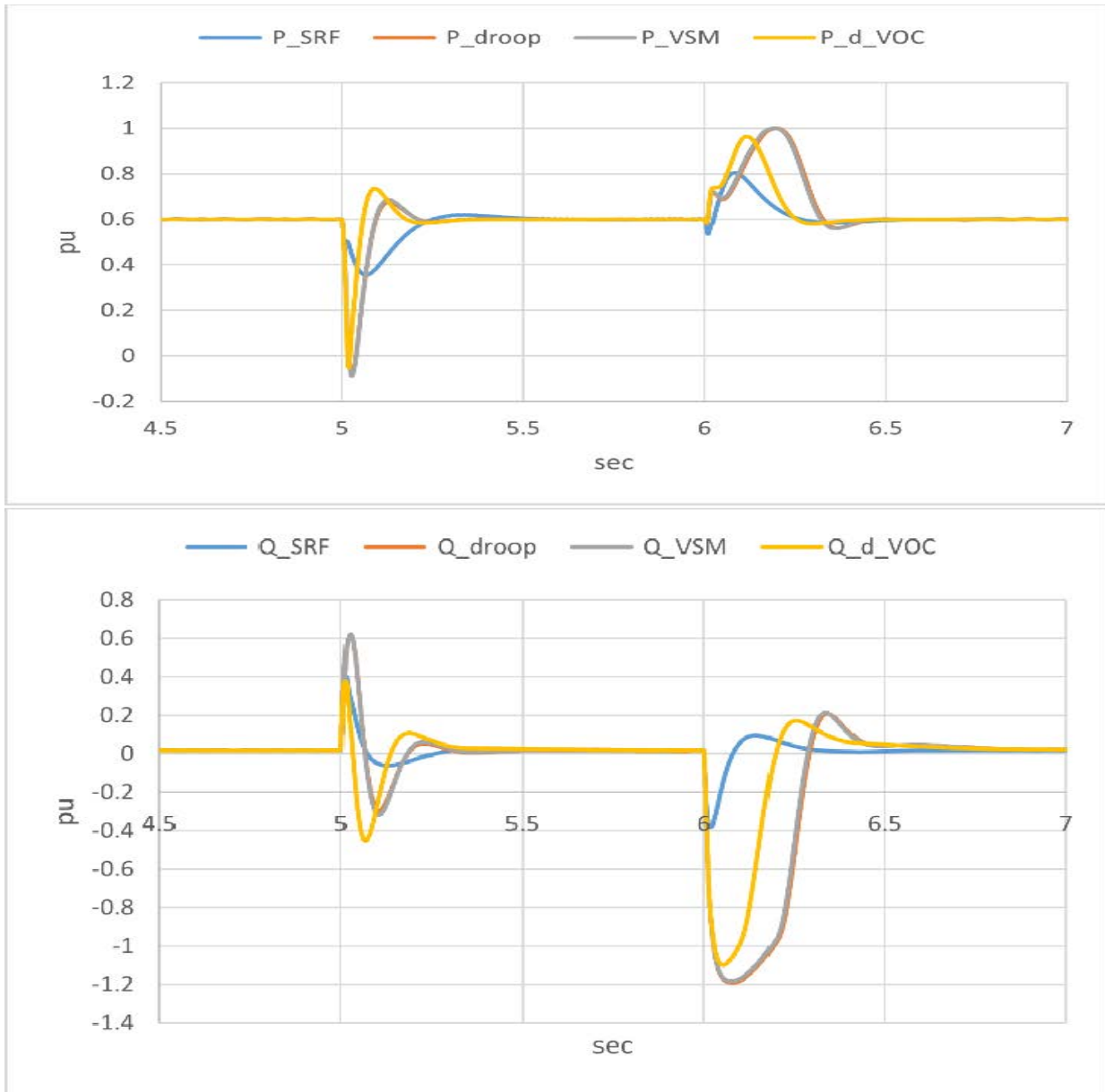


Figure 30. Response of GFM model for balanced positive phase jump when $P = 0.6$ p.u., $Q = 0.1$ p.u.

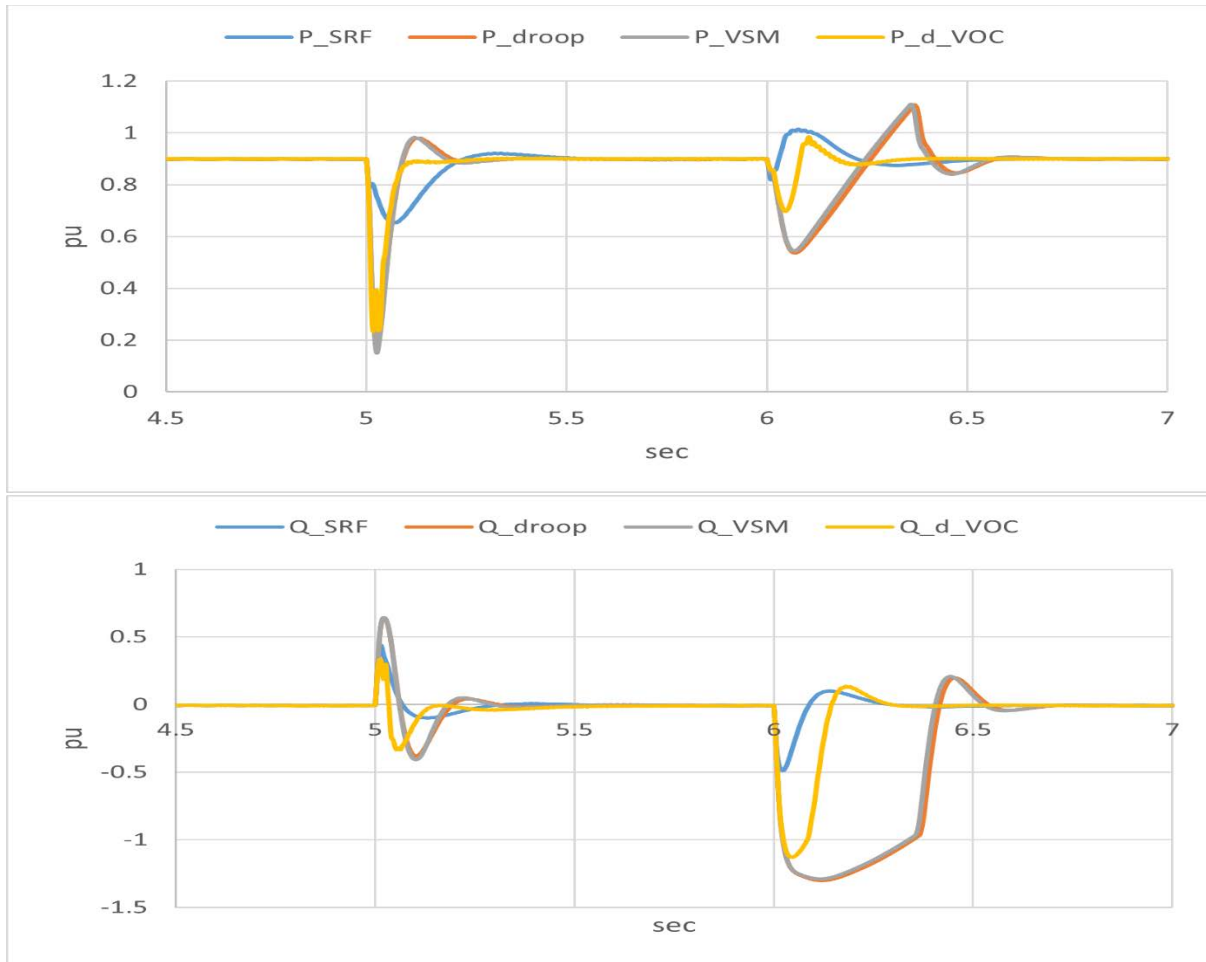


Figure 31. Response of GFM model for balanced positive phase jump when $P = 0.9$ p.u., $Q = 0.2$ p.u.

Unbalanced phase jump of +25 degrees ($P = 0.6$ p.u., $Q = 0.1$ p.u.)

In this test, the phase angle of phase A of system voltage suddenly shifted by +25 degrees at $t = 5$ s. This creates an unbalanced voltage at the POC. At $t = 6$ s, the phase angle of the phase A voltage is returned to the initial condition. Figure 33 and Figure 34 show the response of the GFM model's current. It should be noted that during such unbalances, the negative sequence current increases in response to the negative sequence voltage at the inverter terminal. The results show that the GFM models successfully ride through the phase jump and that the oscillations in the current are positively damped.

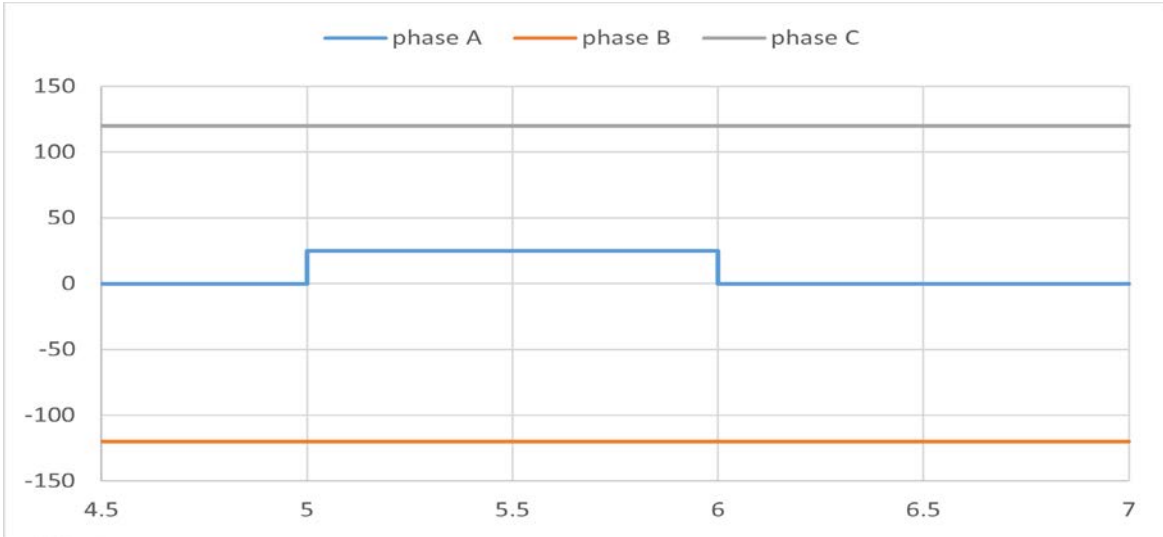


Figure 32. Unbalanced phase jump in applicable voltage

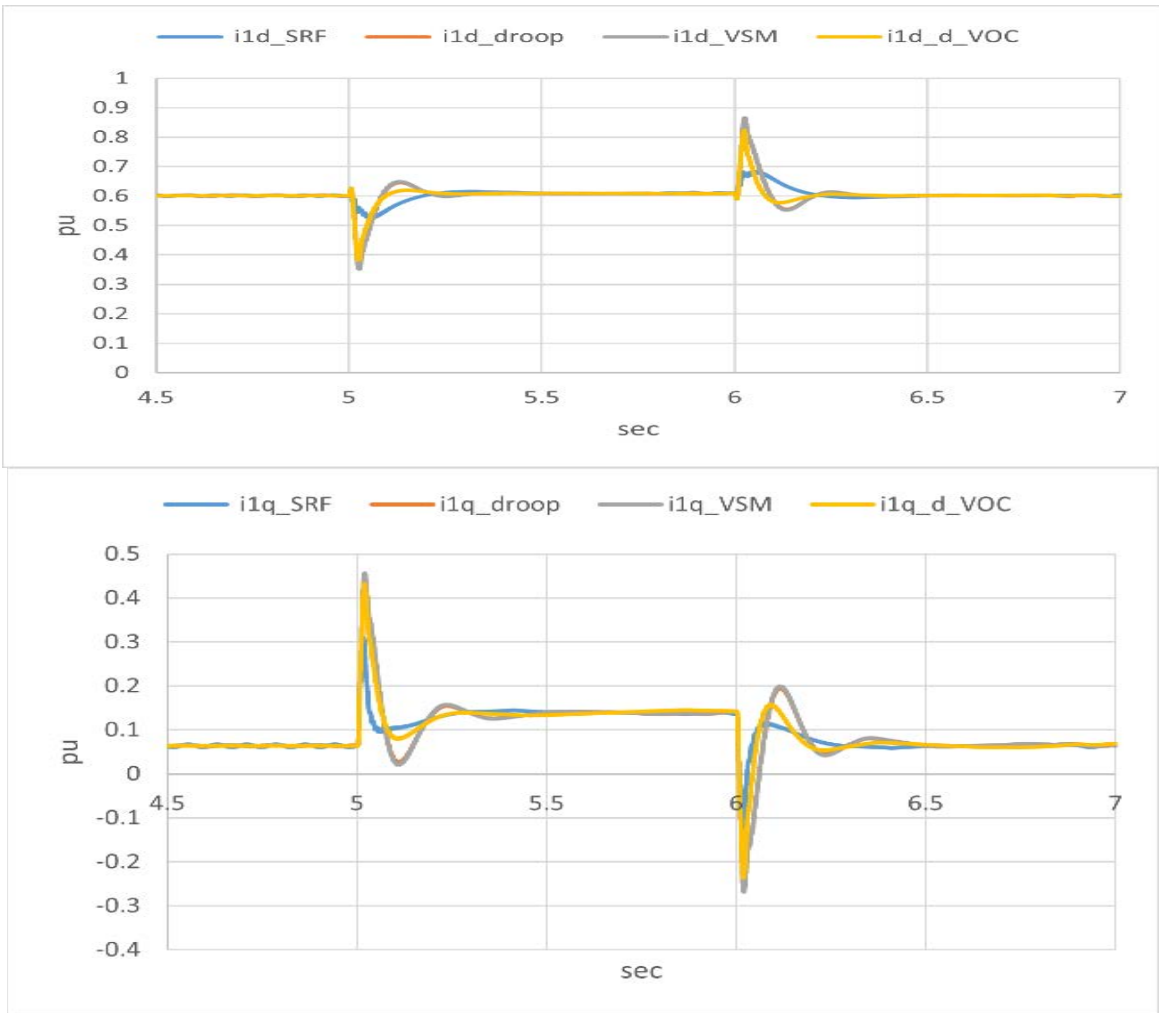


Figure 33. Positive sequence active and reactive current for unbalanced positive phase jump

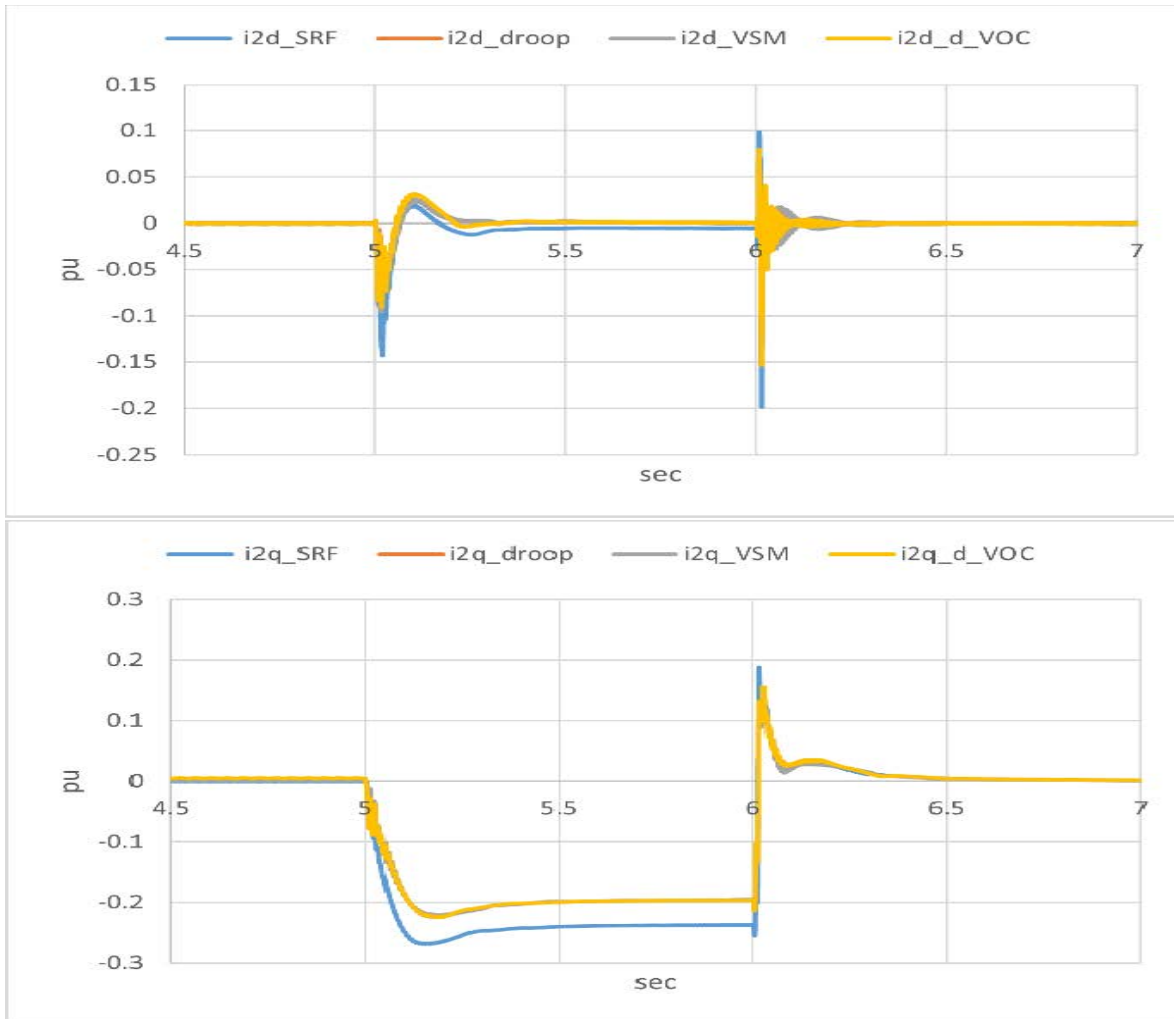


Figure 34. Negative sequence active and reactive current for unbalanced positive phase jump

Unbalanced phase jump of +25 degrees ($P = 0.1$ p.u., $Q = 0.1$ p.u.)

The unbalanced voltage phase angle change is repeated for a different initial operating point. Figure 36 and Figure 37 show the GFM models successfully ride through the phase jump and that the oscillations in the current are positively damped.

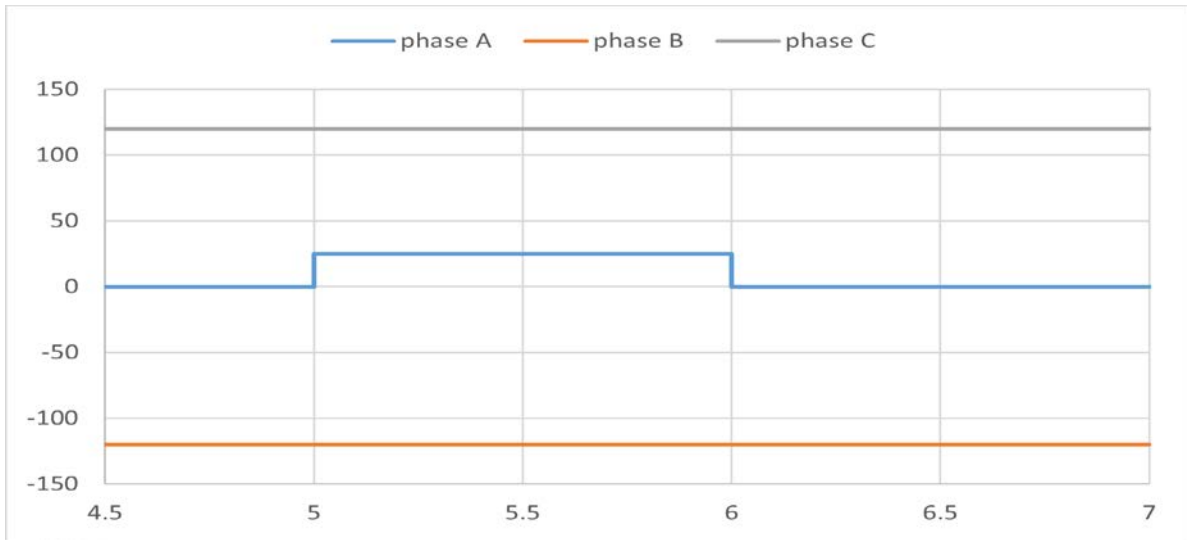


Figure 35. Unbalanced phase jump in applicable voltage when $P = 0.1$ p.u. and $Q = 0.1$ p.u.

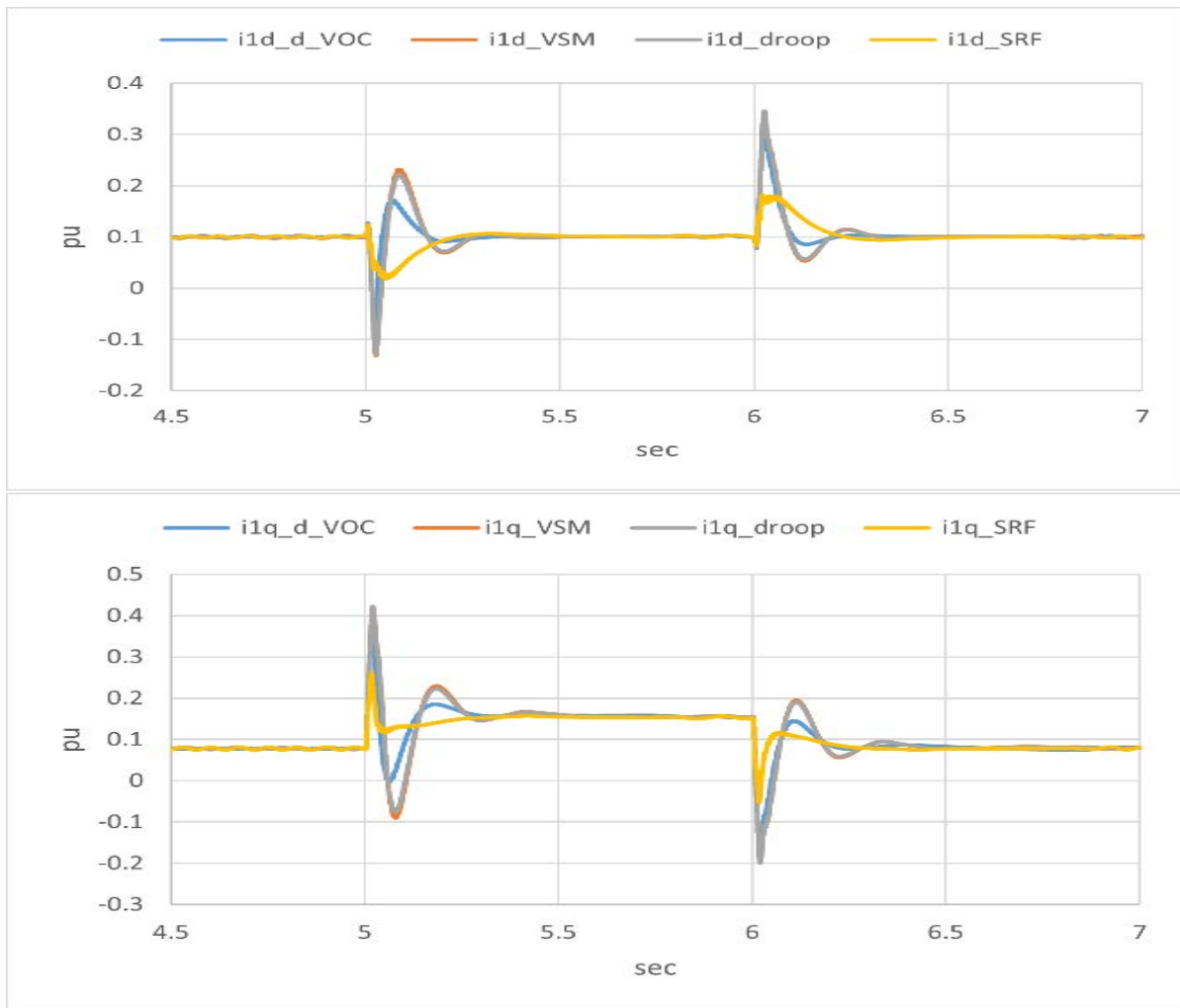


Figure 36. Positive sequence active and reactive current for unbalanced phase jump

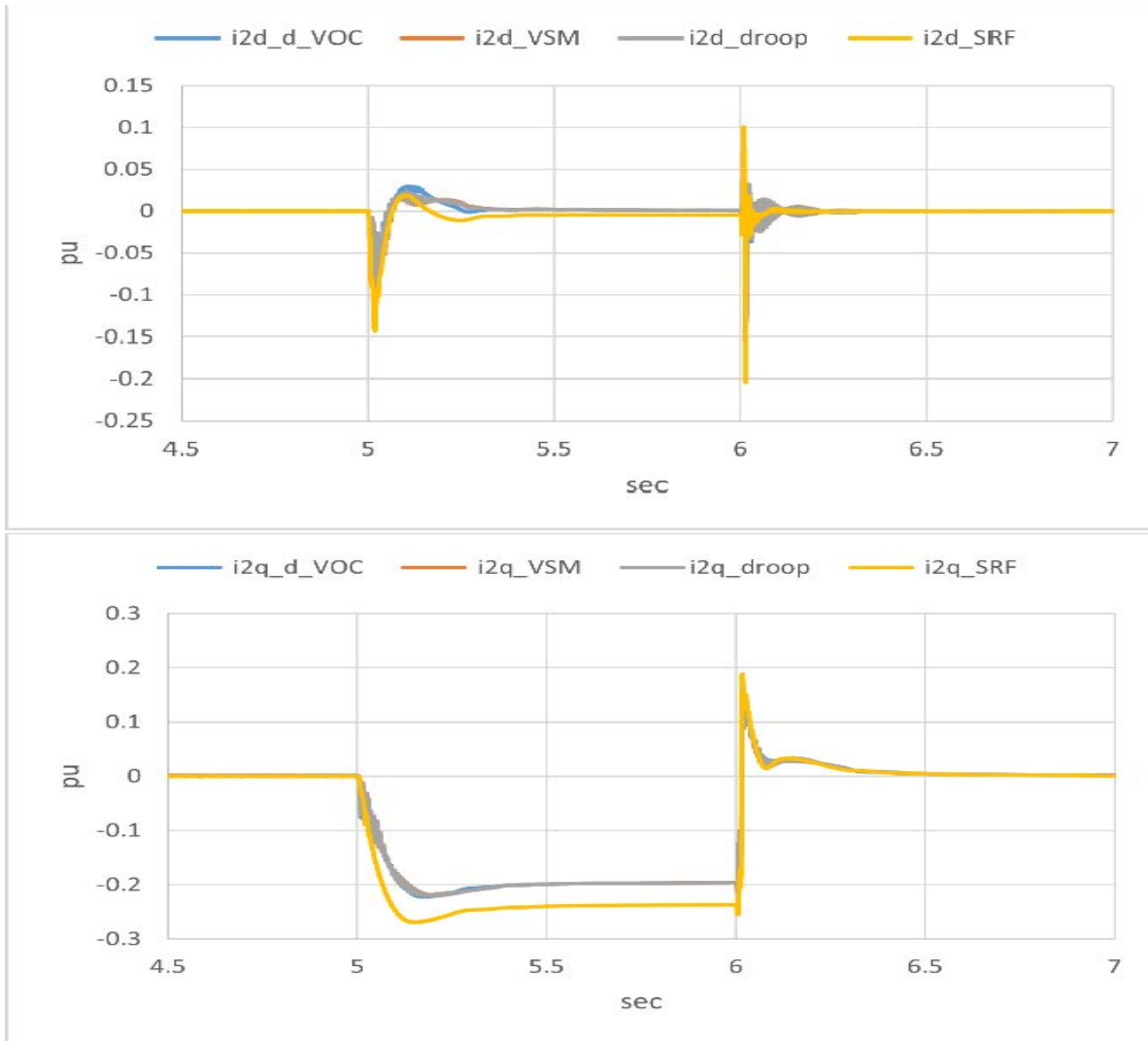


Figure 37. Negative sequence active and reactive current for unbalanced phase jump

Unbalanced phase jump of +25 degrees ($P = 0.9 \text{ p.u.}$, $Q = 0.2 \text{ p.u.}$)

The unbalanced voltage phase angle change is repeated for a different initial operating point. Figure 38 and Figure 39 show the GFM models successfully ride through the phase jump and that the oscillations in the current are positively damped

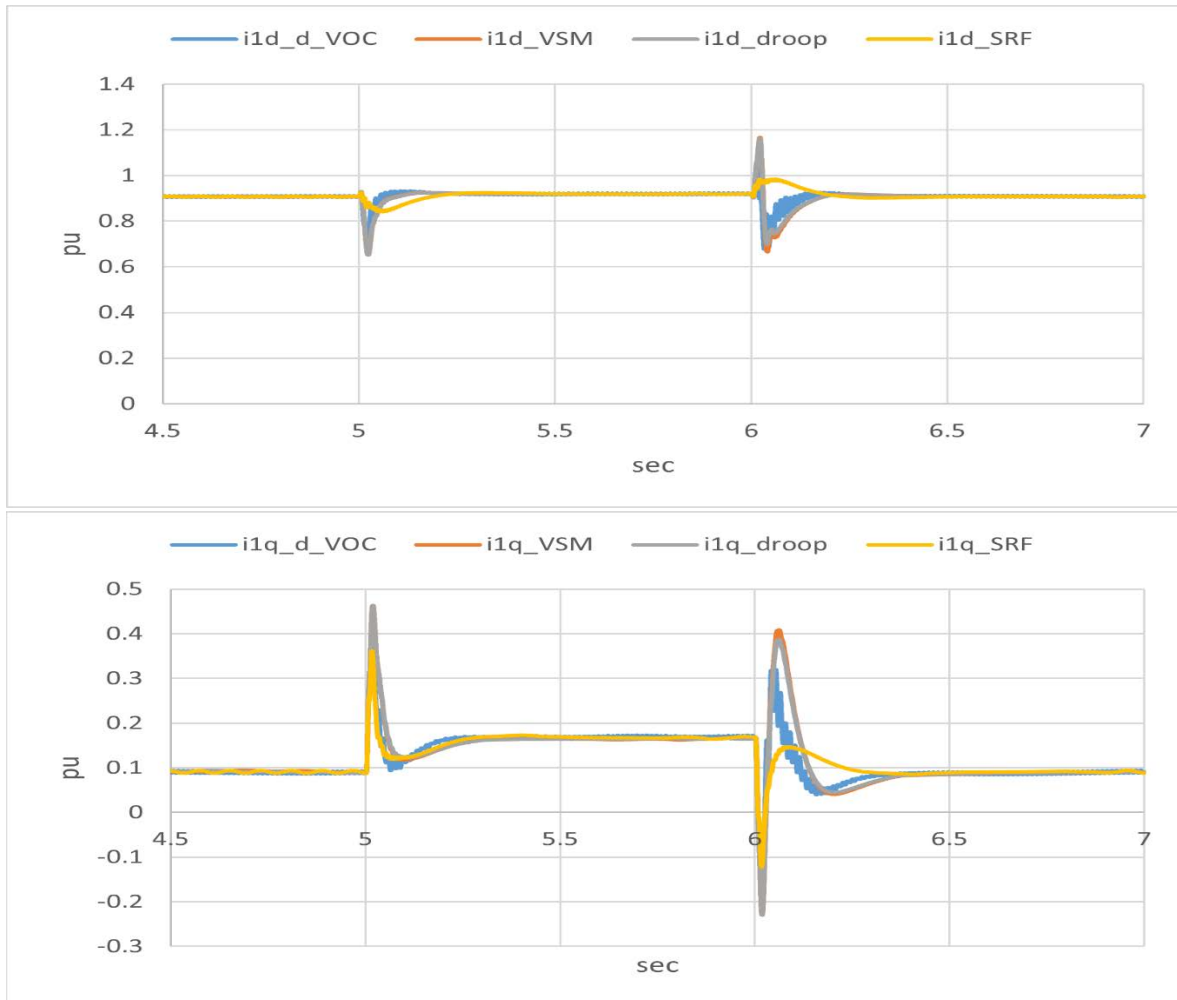


Figure 38. Positive sequence active and reactive current for unbalanced positive phase jump

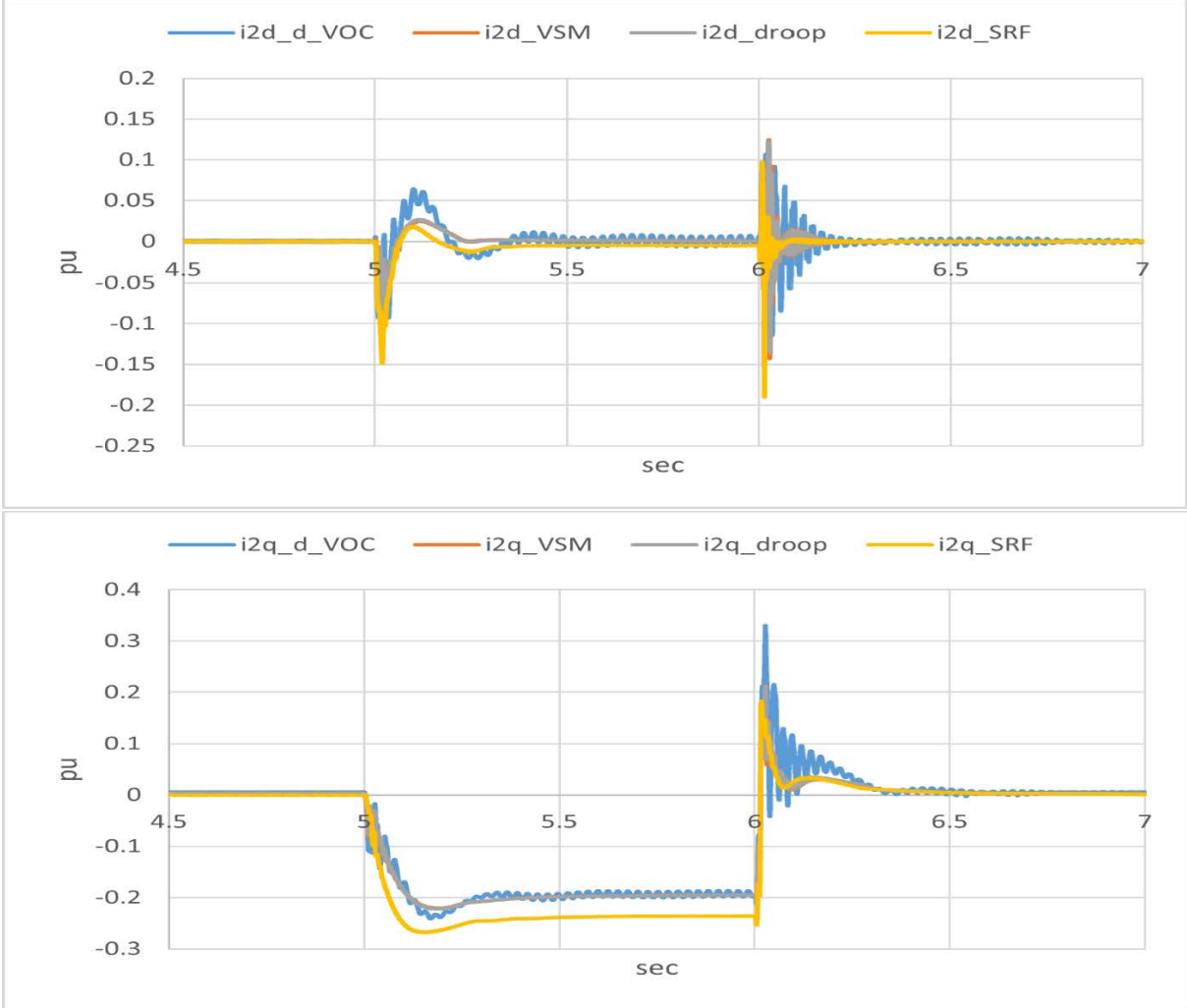


Figure 39. Negative sequence active and reactive current for unbalanced phase jump

Summary

The tests related to volt-var requirements of IEEE Std 1547TM-2018 have revealed that for a voltage disturbance inside the continuous operation region, the response of the generic GFM model is faster compared to the IEEE Std 1547TM-2018 compliant GFL inverter, and faster than what is allowed in IEEE Std 1547TM-2018. For voltage disturbances outside the continuous operation region, the fast response of the GFM model may be allowed by IEEE Std 1547TM-2018 considering the optional dynamic voltage support function defined in the standard. Moreover, the volt-var response curve for the GFM model reveals that the model can effectively limit the reactive power at the inverter terminal than at the RPA (PCC), even though the volt-var operating points of the GFM model are still within the allowable range of IEEE Std 1547TM-2018. For the test related to the frequency droop requirements of IEEE Std 1547TM-2018, the fast response of the GFM model in response to frequency disturbance is allowed by the standard. The steady state frequency watt operating points of the GFM model are also within the allowable range of IEEE Std 1547TM-2018.

For transmission connected IBRs, the tests conducted show that the response of the generic GFM model mostly aligns with the requirements regarding reactive power-voltage control requirement, active power-frequency control requirement, voltage disturbance ride through requirement and phase jump ride through requirement in the IEEE Std TM 2800-2022. However, the rise time and settling time of currents observed for the GFM are larger than the settling time required by the standard for low voltage ride through events. Whether this behavior can be improved, or if a closer look of the requirements in IEEE Std TM 2800-2022 is to be carried out, is a point of discussion. Future tests can also include observation of performance at the current limits and a variety of operational modes. Additionally, in the present set of tests fault ride through behavior has been evaluated by applying a voltage change on the infinite source. In the next round of tests, the behavior would be evaluated through the application of faults.

References

Electric Power Research Institute, "PROPOSAL FOR SUITE OF GENERIC GRID FORMING (GFM) POSITIVE SEQUENCE MODELS," April 2022. [Online]. Available: https://www.wecc.org/_layouts/15/WopiFrame.aspx?sourcedoc=/Administrative/Memo%20on%20Proposal%20for%20Generic%20GFM%20Model_v6_clean.pdf&action=default&DefaultItemOpen=1.



For more information, visit:

www.energy.gov/eere/solar/unifi-consortium